Beer pasteurization models

Kristina Hoffmann Larsen

Kongens Lyngby 2006

IMM-2006-30

Technical University of Denmark
Informatics and Mathematical Modelling
Building 321, DK-2800 Kongens Lyngby, Denmark
Phone +45 45253351, Fax +45 45882673
reception@imm.dtu.dk
www.imm.dtu.dk

Preface

This Master's thesis was completed under the supervision of professor Per Grove Thomsen at the Institute for Informatics and Mathematical Modelling, Technical University of Denmark in co-operation with Sander Hansen A/S.

The work started in September 2005 and ended March 1, 2006.

This thesis has benefited from comments and criticisms of many colleagues and friends. I would like to specially thank Per Grove Thomsen for through guidance and for helping me getting into contact with Sander Hansen. Also the staff at the institute was very helpful by letting me use their computer system and providing me with a place to work.

In addition do that I would like to thank my supervisors at Sander Hansen; Lars Henrik Hansen and Falko Jens Wagner for their guidance and allowing me to use their facilities for experimental purposes.

Lars Gregersen from COMSOL provided wise counsel while I was using COMSOL's program and shall have many thanks for his quick e-mail answers.

Finally I would like to thank my friends and especially my boyfriend who often provided a non-engineering reality check and emotional support during the writing of this thesis.

March 16, 2006 Kristina Hoffmann Larsen
s001584

Abstract

This thesis investigates and develops models for beer pasteurization. There are two different types of models which are used to describe the physics in the pasteurization. The simplest models are developed from general physical considerations which allows a fairly easy implementation in MATLAB. The implementations in MATLAB are examined with the perturbation, initialization and initial guess in mind and hereby allowing determination of whether the results are reliable or not.

The other type of models is more complicated and is generated by using partial differential equations for heat transfer and fluid flow. The models are produced in COMSOL Multiphysics which among many other things allows a visual presentation of the pasteurization process.

To collect the necessary data sets for the models, experiments was made in a small scale pasteurizer located at Sander Hansen's research facility. The data sets from these experiments are used to make the implementation in MATLAB. Furthermore the data sets are used to verify the results from the COMSOL based models.

By using the collected data sets it is possible to investigate the coefficients in the simple models and thereby propose improvements to these models. The data set also made it possible to examine the temperature in the pasteurizer and implement these new results in the models.

In this public version of the thesis 6 sections from the preproject are not included because they contain confidential information. This also means that some expressions in the thesis are rewritten. If you would like to know more about these sections and expressions or if something is difficult to understand because of the missing sections you are welcome to contact Sander Hansen.

On the next page in the section Dansk resumé this abstract can be read in a Danish version.

Dansk resumé

Denne opgave undersøger og udvikler modeller for pasteurisering af øl. Der er to forskelling modeltyper, som bruges til at beskrive fysikken i pasteuriseringen. The simpleste modeller er lavet ud fra generelle fysiske betragtninger, som giver mulighed for en forholdsvis let implementering i MATLAB. Implementeringerne i MATLAB er testede med henblik på perturbation, initialisering og startgæt, og derved gøres det muligt at afgøre, om man kan stole på resultaterne.

Den anden type af modeller er mere komplicerede og er udviklet ved hjælp af partielle differentialligninger for varmeoverførsel og strømninger i væsker. Modellerne er lavet i COMSOL Multiphysics, som blandt andet gøre det muligt at se en visuel præsentation of pasteuriseringsprocessen.

For at samle de nødvendige datasæt til modellerne, blev der lavet eksperimenter i en lille pasteuriseringsmaskine hos Sander Hansen. Datasættene fra disse forsøg bliver brugt til implementeringen i MATLAB. Derudover bruges datasættene til at kontrollere resultaterne fra de COMSOL baserede modeller.

Ved at bruge de indsamlede datasæt bliver det muligt at undersøge koefficienterne i de simple modeller og derved foreslå forbedringer til disse modeller. Datasættene gør det også muligt at undersøge temperaturen i pasteuriseringsmaskinen og implementere disse nye resultater i modellerne.

I denne offentlige version af rapporten er 6 afsnit fra forprojektet udeladt fordi de indeholder fortrolig information. Dette betyder også, at nogle af udtrykkene i rapporten er omskrevet. Hvis du ønsker at vide mere om disse afsnit og udtryk eller hvis noget er svært at forstå på grund af de manglende afsnit er du velkommen til at kontakte Sander Hansen.

Contents

CHAPTER 1

Introduction

This thesis is made after a preceding preparatory project called preproject. The preproject was also written in co-operation with Sander Hansen. Sander Hansen produces pasteurizers for their costumers which are mostly breweries.

It was Sander Hansen who suggested the projects because they wanted to achieve a greater knowledge about the physics in their pasteurization process and examine some aspects in the product model which regulates the pasteurizers. The results should make Sander Hansen able to make a better regulation of the pasteurizers.

The purposes of the preproject was to become acquainted with the present product model and try to develop a new product model which coincide better with the measured values. The highlights from the preproject are described in chapter 2.

The purposes of this thesis are:

- To investigate the sensitivity of the implementation of the product models and the estimation of the parameters and coefficients. The purpose is to find out if the implementation and the results it gives are reliable.
- To investigate the initial guess of the coefficients to make sure that the product models with the final coefficients coincide with the measured values. The purpose is to make sure that the results from an initial guess are reliable.
- To investigate the initialization of the product models in the implementations so that the first steps from the models coincide with the measured values. This is done so the error at the start is as small as possible and the collected error at the end does not stem from an error in the beginning.
- To investigate the temperature which a container experiences while it is transported through the pasteurizer and specially through the gaps. The purpose is to estimate the temperature more precisely and thereby achieve better results for the estimation of the product temperature in the gaps.
- To investigate the coefficients in the product models to find out if they depend on the temperature level and the difference between the spray temperatures in two

neighboring zones. The purpose is to achieve an improved information about the behavior of the product models.

- To investigate the flow and the temperature which occurs inside the container when it is heated/cooled from the outside of the container and hereby see if the flow and temperature depend on the scale of the container. The purpose is to achieve better knowledge about what happens and investigate where in the container the mean product temperature can be measured.

The process of devising this thesis has been a mixture of doing research by the computer and making experiments to collect the necessary data sets to support the theoretical results.

Chapter 2

From Preproject

2.1 The Tunnel Pasteurizers

Sander Hansen's pasteurizers also called pasteurs consist of a tunnel in which there is a belt conveyor. The cans, glass- or PET-bottles, called containers, whose content must be pasteurized are placed on the belt conveyor and are transported through the tunnel. In the tunnel water flows down over the containers, this water is called spray water. The tunnel is divided into several zones, where the spray water has different temperature. Before the water flows down over the containers it is collected in spray pans in the top of the pasteur. Between the spray zones there are small gaps with air to prevent the water and thereby temperature in the different zones to be mixed. Figure 2.1 shows a sketch of a small tunnel pasteur with 5 zones.

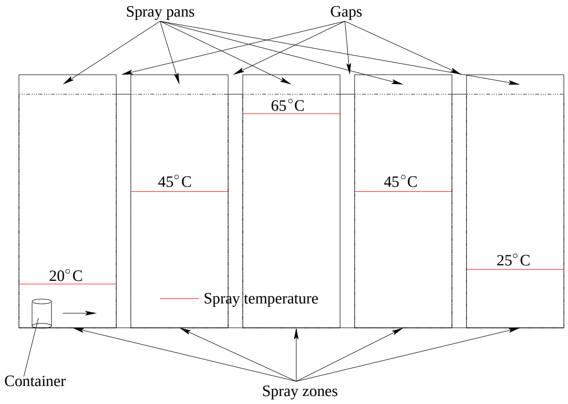

Figure 2.1: Sketch of a tunnel pasteur with 5 spray zones.

The temperatures shown on the figure are only suggested values. The pasteurs which Sander Hansen produces for their costumers are normally between 15 and 30 meters long and have 7 to 15 spray zones. These pasteurs handles between 30000 and 140000 containers per hour. The products are normally beer, soft drinks and juice but also ketchup and canned potatoes are pasteurized in pasteurs produced by Sander Hansen.

First the containers are transported through zones where the temperature of the spray water increases hence the temperature in the product in the containers increases and pasteurization units PU's are obtained.
When the product has obtained the decided number of PU's, the containers are transported through zones where the temperature of the spray water decreases and the product is cooled down. The decided number of PU's is determined by the costumers and depends on the product.
The PU's are calculated by integrating the expression (2.1) with respect to the time t.

$$\frac{dPU}{dt} = 10^{\frac{T-60}{6.94}} \qquad \text{for} \qquad T > T_x \ , \tag{2.1}$$

where T is the temperature in the product and T_x is a temperature decided by the costumer, normally 50°C $\leq T_x \leq$ 58°C. The unit for equation (2.1) is $\left[\frac{PU}{min}\right]$. This means that a product which is 60°C obtain $1PU$ per minute. The temperature in the product and in the container are calculated from a product model which is described on the next pages.

2.2 Conclusion for preproject

The present product model is described and implemented and the implementation gives satisfactory results. The present model has small variations from the measured temperature in the spray zones but by the gaps the variation is larger. A new product model is developed and implemented and the implementation gives better results than the present product model. The variation in the spray zones is almost the same, but the variation by the gaps is smaller. A new spray temperature in the gaps modelled as the spray temperature in the previous zone was tested. For the present model this did not give better results. For the new model the results with the new spray temperature in the gaps gives better results, but the largest variations are still by the gaps. All things considered the purpose of the preproject is fulfilled.

Chapter 3

Test of the implementation

To test whether the implementation of the two product models from the preproject is stable and gives good and reliable results, two important parts of the implementation are investigated: If the results changes if the perturbation, when finding the Jacobian matrix, is changed to a smaller or larger value, and if the results changes if the initial value for the coefficients is changed. Additionally it is examined why the implementation gives the same temperature in the first two time steps. Before this investigation the general sensitivity of the product models is tested.

3.1 Sensitivity of the present product model

Both expressions in the present product model are functions of two temperatures, the time step and a coefficient

$$T_{1,new} = T_{1,new}(T_2, T_{1,old}, c, dt) \ , \tag{3.1}$$

where c is the coefficient, $0 < c < 1$ and dt is the time step, $dt > 0$. In the implementation dt is constant. To see how the model behaves when the coefficients are changed, the behavior of $T_{1,new}$ is investigated as a function of c for different constant $T_{1,old}$.

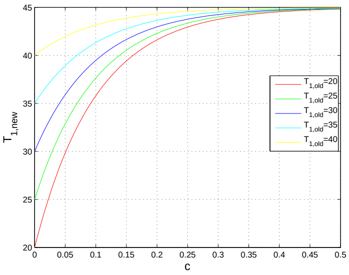

Figure 3.1: $T_{1,new}$ as a function of c for constant $dt = 10$ and $T_2 = 45$ for 5 different values of $T_{1,old} = 20$, 25, 30, 35 and 40.

In the example on figure 3.1 $T_2 = 45$, $dt = 10$ and $T_{1,old}$ is 20, 25, 30, 35 and 40. From $0.5 < c < 1$ the value of $T_{1,new}$ gets closer and closer to 45. As it can be seen very small changes in c only costs small changes in $T_{1,new}$. The smaller the difference between T_2 and $T_{1,old}$ is the less a change in c will affect $T_{1,new}$. The larger c is the less a change in c will affect $T_{1,new}$.

3.2 Sensitivity of the new product model

The new product model also consists of to expressions. One of them is the same as the expressions from the present model and therefore the behavior is like the present product model. The other expression is a function of three temperatures, the time step and 3 coefficients

$$T_{1,new} = T_{1,new}(T_{1,old}, T_2, T_3, c, C_1, C_2, dt) \ , \tag{3.2}$$

where c, C_1 and C_2 are the coefficient, $0 < c < 1$ and dt is the time step, $dt > 0$. In the implementation dt is constant. The behavior of expression (3.2) with respect to the 3 coefficients c, C_1 and C_2 is investigated in two steps. First the dependency of the coefficient c is examined by taking the other coefficients to be constant $C_1 = 0.9$ and $C_2 = 1 - C_1 = 0.1$. $T_2 = 45$ and $dt = 10$. $T_{1,new}$ is plotted as a function of c for 5 different values of $T_{1,old} = 20$, 25, 30, 35 and 40 . On figure 3.2 $T_3 = 20$ and on figure 3.3 $T_3 = 35$.

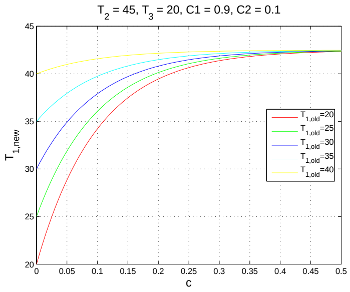

Figure 3.2: $T_{1,new}$ as a function of c for constant $C_1 = 0.9$, $C_2 = 0.1$, $dt = 10$, $T_2 = 45$ and $T_3 = 20$ for 5 different values of $T_{1,old} = 20$, 25, 30, 35 and 40.

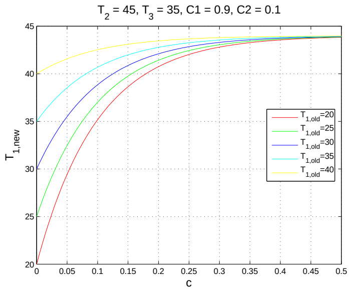

Figure 3.3: $T_{1,new}$ as a function of c for constant $C_1 = 0.9$, $C_2 = 0.1$, $dt = 10$, $T_2 = 45$ and $T_3 = 35$ for 5 different values of $T_{1,old} = 20$, 25, 30, 35 and 40.

The two figures are very similar and also similar to figure 3.1. It can be seen on both of them that small changes in c only costs small changes in $T_{1,new}$. The smaller the difference between T_2 and $T_{1,old}$ is the less a change in c will affect $T_{1,new}$. The larger c is the less a change in c will affect $T_{1,new}$. The difference in T_3 in the two figures does not have very big influence.

The dependency on C_1 and C_2 is examined by taking $c = 0.01$ constant and plotting $T_{1,new}$ as a function of C_1 for the same 5 different values of $T_{1,old}$. On figure 3.4 $T_3 = 20$ and on figure 3.5 $T_3 = 35$.

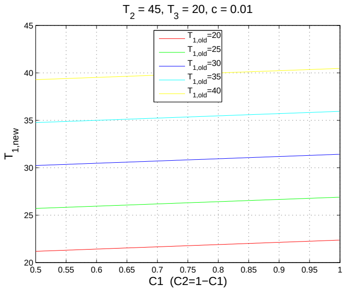

Figure 3.4: $T_{1,new}$ as a function of C_1 for constant $c = 0.01$, $dt = 10$, $T_2 = 45$ and $T_3 = 20$ for 5 different values of $T_{1,old} = 20, 25, 30, 35$ and 40.

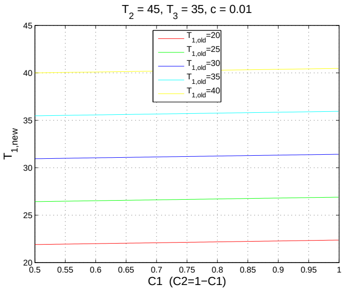

Figure 3.5: $T_{1,new}$ as a function of C_1 for constant $c = 0.01$, $dt = 10$, $T_2 = 45$ and $T_3 = 35$ for 5 different values of $T_{1,old} = 20, 25, 30, 35$ and 40.

The two figures looks similar and a small change in C_1 does not affect $T_{1,new}$ very much. A change in C_1 gives the same change in $T_{,new}$ no matter what the difference between $T_{1,new}$ and T_2 are, there is a linear dependency on C_1 when c, $T_{1,old}$, T_2 and T_3 are constant. The difference in T_3 in the two figures does only have a very small influence and can almost not be seen on the figures.

3.3 General for both product models

Both product models are only affected a little by small changes in the constants. When the residue is found in the implementation it normally lies in an interval with a range of approximately 3.5 ℃. This means that when two residues from the same data set, but with different perturbation or initial value for the coefficients, is compared the maximum absolute difference between the two residues should to be in the order of 10^{-2} because when this is the case the difference can not be seen on the graph and it is less than 1.5% of the residue. Two residues from the same model and with same data set but with different perturbations or initial values of the coefficients which fulfill this can be assumed to be the same and thereby the measured temperatures can be assumed to be the same.
From each data set approximately 300 interconnected values of t, T_s and T_p are used. This means that each residue and absolute difference between two residues also consists of approximately 300 values. If each of the 300 values in the absolute difference are less than or equal to a value in the order of 10^{-2} the sum of the absolute difference between two residues is less than 15. 15 is the worst case limit where all 300 values are equal to $5 \cdot 10^{-2}$, so in most cases the sum of the absolute difference will be much less than 15.

3.4 Test of perturbation in present product model

The perturbation in the implementation of the present product model is tested by choosing a small perturbation as a reference perturbation and then compare the results for this perturbation with the results for 8 different larger perturbations. This is repeated for different data sets. The reference perturbation is set to 0.00001 and the other 8 perturbations $pertub$ is 0.00005, 0.0001, 0.0005, 0.001, 0.005, 0.01, 0.05 and 0.1. The initial values for the coefficients are the same for each perturbation and each data set. The results that are tested are the absolute difference between the final coefficients for the reference perturbation and the final coefficients for each of the other perturbations $|\Delta coe|$, the sum of the absolute difference between the final residue for the reference perturbation and the final residue for each of the other perturbations $\sum|\Delta res|$ and the maximum value of the absolute difference between the final residue for the reference perturbation and the final residue for each of the other perturbations $\max|\Delta res|$. The number of iterations $\#it$ for each perturbation is also recorded to make sure that the implementation converge for each perturbation. The perturbation is tested for 26 different data sets and the results for all of them looks the same and are similar to the results in the tables 3.1 and 3.2 which is for the two data sets `m824cs.m` and `m824rd.m`.

	$pertub$	$\sum\|\Delta res\|$	$\max\|\Delta res\|$	$\|\Delta coe\|$	$\#it$
`m824cs.m`					
	0.00005	0.0024	$2.0725 \cdot 10^{-5}$	$10^{-4} \cdot$ [0.0001 0.0008 ... 0.0006 0.0001 0.4075]	34
	0.0001	0.0053	$4.6623 \cdot 10^{-5}$	$10^{-4} \cdot$ [0.0002 0.0018 ... 0.0013 0.0003 0.9161]	34
	0.0005	0.0288	$2.5372 \cdot 10^{-4}$	$10^{-3} \cdot$ [0.0001 0.0010 ... 0.0007 0.0002 0.4991]	34
	0.001	0.0582	$5.1232 \cdot 10^{-4}$	$10^{-2} \cdot$ [0.0000 0.0002 ... 0.0001 0.0000 0.1008]	34
	0.005	0.2921	$2.5699 \cdot 10^{-3}$	$10^{-2} \cdot$ [0.0001 0.0010 ... 0.0007 0.0002 0.5094]	34
	0.01	0.5810	$5.1144 \cdot 10^{-3}$	$10^{-1} \cdot$ [0.0000 0.0002 ... 0.0001 0.0000 0.1022]	34
	0.05	2.2408	$2.3110 \cdot 10^{-2}$	$10^{-1} \cdot$ [0.0001 0.0009 ... 0.0007 0.0001 0.5201]	33
	0.1	3.6663	$4.3193 \cdot 10^{-2}$	[0.0000 0.0002 ... 0.0001 0.0000 0.1049]	31

Table 3.1: Results in the present product model of the test of the perturbation. Reference perturbation = 0.00001.

It can be seen that the results increases as the perturbation increases. In table 3.1 and table 3.2 all the perturbations can be used because all values of $\max|\Delta res|$ are smaller than or in the order of 10^{-2}. This is the case for 25 out of the 26 data sets, in the last data set the value of $\max|\Delta res|$ for the largest perturbation is in the order of 10^{-1}, so this perturbation is to large. The values of $\sum|\Delta res|$ for all perturbations and all data sets are

	$pertub$	$\sum \lvert\Delta res\rvert$	$\max \lvert\Delta res\rvert$	$\lvert\Delta coe\rvert$	$\#it$
`m824rd.m`					
	0.00005	0.0023	$1.7135 \cdot 10^{-5}$	$10^{-5} \cdot$ [0.0009 0.1411 ... 0.0043 0.0009 0.2908]	31
	0.0001	0.0052	$3.8566 \cdot 10^{-5}$	$10^{-5} \cdot$ [0.0019 0.3176 ... 0.0097 0.0019 0.6546]	31
	0.0005	0.0281	$2.1003 \cdot 10^{-4}$	$10^{-4} \cdot$ [0.0011 0.1729 ... 0.0053 0.0011 0.3563]	31
	0.001	0.0568	$4.2418 \cdot 10^{-4}$	$10^{-4} \cdot$ [0.0021 0.3488 ... 0.0106 0.0021 0.7102]	31
	0.005	0.2760	$2.1044 \cdot 10^{-3}$	$10^{-3} \cdot$ [0.0009 0.1367 ... 0.0048 0.0011 0.3486]	31
	0.01	0.5017	$3.5519 \cdot 10^{-3}$	$10^{-3} \cdot$ [0.0017 0.1833 ... 0.0045 0.0019 0.4911]	31
	0.05	2.4912	$1.8067 \cdot 10^{-2}$	$10^{-2} \cdot$ [0.0009 0.1331 0.0032 0.0009 0.2629]	31
	0.1	4.6610	$3.3629 \cdot 10^{-2}$	$10^{-2} \cdot$ [0.0018 0.2498 ... 0.0058 0.0018 0.4694]	31

Table 3.2: Results in the present product model of the test of the perturbation. Reference perturbation = 0.00001.

much smaller than the worst case limit on 15. The number of iterations for each data set is almost the same for all perturbations. This means that all perturbations between 0.00005 and 0.05 can be used. If the perturbation is 0.001, as it was in the implementations in the preproject, the values of $\max|\Delta res|$ are in the order between 10^{-5} and 10^{-3} and most of them are in the order of 10^{-4} which are 10^2 times smaller than the limit. The values of $|\Delta coe|$ are all very small except for the last coefficient for $pertub = 0.1$ for the data set `m824cs.m` which value is approximately 0.1. The final coefficients for the data set `m824cs.m` with the reference perturbation are [0.0041 0.0152 0.0038 0.0052 0.3883], so according to section 3.1 a change by 0.1 will almost not affect the temperature when the coefficient is 0.3883.

3.5 Test of initial values for coefficients in present model

The initial values for each of the coefficients in the implementation of the present product model are tested by taking a initial value which gives good results as a reference initial value and then compare the results for this initial value with the results for other initial values. The test is made to find an interval for the initial value for each coefficient by trying different combinations and then examine the results. If a value gives a good result the interval is made larger and if the results are not good the interval is made smaller. The results that are tested are the absolute difference between the final coefficients for the reference initial value and the final coefficients for each of the other initial values $|\Delta coe|$, the sum of the absolute difference between the final residue for the reference initial value and the final residue for each of the other initial values $\sum |\Delta res|$ and the maximum value of the absolute difference between the final residue for the reference initial value and the final residue for each of the other initial values $\max |\Delta res|$. The number of iterations $\#it$ for each initial value is also recorded to make sure that the implementation converge for each initial value. The intervals are found from testing 6 data sets and are found to

$$\begin{aligned} 0.004 \leq & c_1 \leq 0.01 \\ 2c_1 \leq & c_2 \leq 10c_1 \\ 0 < & c_3 \leq 0.04c_2 \\ 0.003 \leq & c_4 \leq 0.01 \\ & c_5 \approx 2c_4 \ , \end{aligned} \tag{3.3}$$

where $coe = [c_1\ c_2\ c_3\ c_4\ c_5]$. To test these limits on more data sets the initials values in table 3.3 are tested on 26 data sets. Initial value No. 1 is used as the reference initial value.

Initial value No.	initial value
1	[0.004 0.008 0.002 0.004 0.008]
2	[0.01 0.02 0.002 0.004 0.008]
3	[0.004 0.1 0.002 0.004 0.008]
4	[0.004 0.008 0.00000000002 0.004 0.008]
5	[0.004 0.008 0.0032 0.004 0.008]
6	[0.004 0.008 0.002 0.003 0.006]
7	[0.004 0.008 0.002 0.01 0.02]

Table 3.3: Initial values used for the present product model for the test of initial values.

All data sets give results similar to the results in the tables 3.4 and 3.5 which are for the data sets `m824cs.m` and `m824rd.m`.
It can be seen that all the values of $\max |\Delta res|$ in the table are in the order of 10^{-2} or less and all values of $\sum |\Delta res|$ are much less than the worst case limit on 15. This is also the case for all the other 24 data sets. The values of $|\Delta coe|$ are all very small except for the last coefficient for the initial value No. 2, 6 and 7 for the data set `m824cs.m`. These values are approximately 0.1 or 0.3. The last coefficients for the data set `m824cs.m` with the reference initial value is 0.3883, so according to section 3.1 a change by 0.1 or 0.3 will almost not affect the temperature when the coefficient is 0.3883. This means that all data sets gives good results if the initial values for the coefficients are inside the intervals.

	Iv No.	$\sum \lvert \Delta res \rvert$	$\max \lvert \Delta res \rvert$	$\lvert \Delta coe \rvert$	$\#it$
`m824cs.m`					
	2	2.2010	$1.1873 \cdot 10^{-2}$	$10^{-1} \cdot$ [0.0001 0.0001 ... 0.0001 0.0001 0.1822]	36
	3	1.6297	$1.5271 \cdot 10^{-2}$	[0.0000 0.0000 ...] 0.0001 0.0000 0.1054	35
	4	0.3141	$6.0653 \cdot 10^{-3}$	$10^{-1} \cdot$ [0.0000 0.0000 ...] 0.0002 0.0000 0.4971	34
	5	0.0688	$7.5293 \cdot 10^{-4}$	$10^{-2} \cdot$ [0.0000 0.0001 ... 0.0001 0.0000 0.4746]	34
	6	1.5601	$1.4178 \cdot 10^{-2}$	[0.0000 0.0000 ... 0.0000 0.0000 0.2509]	39
	7	3.1420	$3.5182 \cdot 10^{-2}$	[0.0000 0.0000 ... 0.0000 0.0000 0.1088]	33

Table 3.4: Results of the test of the initial values in the present product model. Reference initial value No. 1 = [0.004 0.008 0.002 0.004 0.008].

	Iv No.	$\sum \lvert \Delta res \rvert$	$\max \lvert \Delta res \rvert$	$\lvert \Delta coe \rvert$	$\#it$
`m824rd.m`					
	2	6.8382	$5.2126 \cdot 10^{-2}$	$10^{-2} \cdot$ [0.0030 0.2019 ... 0.0062 0.0002 0.1927]	28
	3	3.7819	$2.1604 \cdot 10^{-2}$	$10^{-3} \cdot$ [0.0060 0.2868 ... 0.0153 0.0050 0.7657]	27
	4	0.8187	$6.2802 \cdot 10^{-3}$	$10^{-3} \cdot$ [0.0032 0.1946 ... 0.0097 0.0009 0.2776]	32
	5	0.1298	$1.2345 \cdot 10^{-3}$	$10^{-3} \cdot$ [0.0002 0.0472 ... 0.0042 0.0003 0.1154]	31
	6	1.9842	$2.0968 \cdot 10^{-2}$	$10^{-3} \cdot$ [0.0002 0.1782 ... 0.0073 0.0073 0.2518]	31
	7	3.7563	$3.3246 \cdot 10^{-2}$	$10^{-2} \cdot$ [0.0001 0.0088 ... 0.0047 0.0013 0.2082]	32

Table 3.5: Results of the test of the initial values in the present product model. Reference initial value No. 1 = [0.004 0.008 0.002 0.004 0.008].

3.6 Test of perturbation in new product model

The perturbation in the implementation of the new product model is tested in the same way as the present model and the same results are investigated. The data sets used to test the new product model are also the same. The results are more dissimilar for the new model but there are still some similarities. All data sets can not converge for the two largest perturbations 0.05 and 0.1 so these perturbations are to large. Some of the data sets can also not converge for the third largest perturbation 0.01 so this perturbation is also to large. Finally a few of the data sets can not converge for some random perturbations this is the case if the data set has some irregularities in the measured product temperature.

The results of the converging data sets for the 5 smallest perturbations have the same tendency as the results for the present model namely that the values increases as the perturbation increases. But the difference between the values for different data sets varies more. In the tables 3.6 and 3.7 the result for the two data sets `m824cs.m` and `m824rd.m` are shown.

	pertub	$\sum \lvert\Delta res\rvert$	$\max \lvert\Delta res\rvert$	$\lvert\Delta coe\rvert$	$\#it$
`m824cs.m`					
	0.00005	0.0169	$2.6775 \cdot 10^{-4}$	$10^{-2} \cdot$ [0.0001 0.0001 0.0000 ... 0.0010 0.0078 0.0034 0.0002 ... 0.0125 0.0126 0.1084 0.1070]	516
	0.0001	0.1181	$4.2304 \cdot 10^{-3}$	$10^{-2} \cdot$ [0.0012 0.0009 0.0014 ... 0.0029 0.0952 0.0500 0.0030 ... 0.3426 0.3509 0.3256 0.3215]	530
	0.0005	0.0897	$1.6015 \cdot 10^{-3}$	$10^{-1} \cdot$ [0.0002 0.0002 0.0001 ... 0.0014 0.0012 0.0043 0.0033 ... 0.00507 0.0517 0.1509 0.1491]	524
	0.001	0.1239	$2.5845 \cdot 10^{-3}$	$10^{-1} \cdot$ [0.0003 0.0002 0.0000 ... 0.0029 0.0045 0.0030 0.0022 ... 0.0719 0.0733 0.3021 0.2985]	525
	0.005	20.5876	$7.9977 \cdot 10^{-1}$	[0.0004 0.0002 0.0006 ... 0.4313 0.3158 0.0289 0.0021 ... 0.1277 0.1317 0.7525 0.7426]	601
	0.01	31.6941	1.0009	[0.0002 0.0000 0.0002 ... 0.4949 0.3847 0.0377 0.0490 ... 0.0585 0.0609 0.7596 0.7489]	599
	0.05	111.6186	2.3231	[0.0042 0.0031 0.0047 ... 1.1238 1.0160 7.5089 7.8489 ... 0.4583 0.4697 0.7920 0.7775]	3000
	0.1	100.3573	2.0248	[0.0022 0.0020 0.0048 ... 1.0985 0.9910 8.7916 9.0318 ... 0.3318 0.3372 0.7877 0.7738]	3000

Table 3.6: Results in the new product model of the test of the perturbation. Reference perturbation = 0.00001.

	$pertub$	$\sum \lvert \Delta res \rvert$	$\max \lvert \Delta res \rvert$	$\lvert \Delta coe \rvert$	$\#it$
`m824rd.m`					
	0.00005	0.0034	$5.6331 \cdot 10^{-5}$	$10^{-3} \cdot$ [0.0004 0.0010 0.0001 ... 0.0007 0.0143 0.0090 0.0090 ... 0.0538 0.0542 0.1631 0.1710]	322
	0.0001	0.0063	$1.1162 \cdot 10^{-4}$	$10^{-3} \cdot$ [0.0009 0.0016 0.0000 ... 0.0016 0.0047 0.0060 0.0069 ... 0.1151 0.1164 0.3672 0.3840]	322
	0.0005	0.0726	$5.9105 \cdot 10^{-4}$	$10^{-2} \cdot$ [0.0005 0.0013 0.0001 ... 0.0009 0.0134 0.0075 0.0078 ... 0.0655 0.0660 0.2007 0.2109]	323
	0.001	0.1065	$2.8883 \cdot 10^{-3}$	$10^{-2} \cdot$ [0.0012 0.0034 0.0005 ... 0.0019 0.0600 0.0467 0.0438 ... 0.1418 0.1425 0.4121 0.4333]	322
	0.005	0.5941	$1.6974 \cdot 10^{-2}$	$10^{-1} \cdot$ [0.0007 0.0015 0.0004 ... 0.0011 0.0352 0.0265 0.0242 ... 0.0803 0.0809 0.2404 0.2553]	321
	0.01	49.7581	$8.862 \cdot 10^{-1}$	[0.0004 0.0087 0.0015 ... 0.7824 0.6957 0.2919 0.3495 ... 0.0382 0.0371 0.8399 0.8634]	923
	0.05	89.9720	1.3023	[0.0053 0.0177 0.0023 ... 0.7597 0.6759 0.2295 0.2917 ... 0.3016 0.2995 0.8465 0.8688]	3000
	0.1	101.9661	1.5011	[0.0801 0.0433 0.0020 ... 1.0492 0.7615 0.2080 1.2249 ... 0.5013 0.7075 0.8212 0.8485]	3000

Table 3.7: Results in the new product model of the test of the perturbation. Reference perturbation = 0.00001.

For *pertub* = 0.005 most of the maximum values of the difference of the residuals is of order of 10^{-1} and the other varies in the order of $10^{-3} - 1$. For *pertub* = 0.001 most of the maximum values of the difference of the residuals is of order of 10^{-3} and the other varies in the order of $10^{-4} - 10^{-1}$. The sum of the absolute difference of the residues is in most cases much smaller than the worst case limit on 15 when the perturbation is equal to 0.001. For perturbations equal to 0.005 this sum is in some cases larger than the limit on 15. This means that a perturbation equal to 0.001 is a good choice in many cases and that *pertub* = 0.005 is to large. If *pertub* = 0.001 does not give nice results the value of the perturbation can be decreased.

3.7 Test of initial values for coefficients in new model

The initial values for the coefficients in the implementation of the new product model are tested in the same way as the present model. The new product model contains 11 coefficients $coe = [c_1\ c_2\ c_3\ c_4\ c_5\ c_6\ c_7\ c_8\ c_9\ c_{10}\ c_{11}]$, $c_1 - c_5$ correspond to the coefficients from the present model and $c_6 - c_{11}$ are the new coefficients. The initial values for the new coefficients fulfills the conditions $c_6 = c_8 = c_{10}$, $c_7 = c_9 = c_{11}$ and $c_6 + c_7 = 1$, $c_8 + c_9 = 1$, $c_{10} + c_{11} = 1$. The intervals are found from the 6 same data sets as the intervals for the present model. The intervals are

$$\begin{aligned}
0.003 \leq &c_1 \leq 0.009 \\
&c_2 \approx 2c_1 \\
0 < &c_3 \leq 0.0022 \\
0.003 \leq &c_4 \leq 0.007 \\
2c_4 \leq &c_5 \leq 0.014 \\
0.89 \leq &c_6 \leq 0.91 \\
0.17 \leq &c_7 \leq 0.11 \\
0.89 \leq &c_8 \leq 0.91 \\
0.17 \leq &c_9 \leq 0.11 \\
0.89 \leq &c_{10} \leq 0.91 \\
0.17 \leq &c_{11} \leq 0.11
\end{aligned} \tag{3.4}$$

To test these limits on more data sets 26 data sets are tested with all the initial values in table 3.8. Initial value No. 1 is used as the reference initial value.

Initial value No.	initail value
1	[0.004 0.008 0.002 0.004 0.008 0.9 0.1 0.9 0.1 0.9 0.1]
2	[0.003 0.006 0.002 0.004 0.008 0.9 0.1 0.9 0.1 0.9 0.1]
3	[0.009 0.018 0.002 0.004 0.008 0.9 0.1 0.9 0.1 0.9 0.1]
4	[0.004 0.008 0.00000000002 0.004 0.008 0.9 0.1 0.9 0.1 0.9 0.1]
5	[0.004 0.008 0.0022 0.004 0.008 0.9 0.1 0.9 0.1 0.9 0.1]
6	[0.004 0.008 0.002 0.003 0.008 0.9 0.1 0.9 0.1 0.9 0.1]
7	[0.004 0.008 0.002 0.007 0.014 0.9 0.1 0.9 0.1 0.9 0.1]
8	[0.004 0.008 0.002 0.004 0.008 0.91 0.09 0.91 0.09 0.91 0.09]
9	[0.004 0.008 0.002 0.004 0.008 0.89 0.11 0.89 0.11 0.89 0.11]

Table 3.8: Initial values used for the new product model for the test of initial values.

Most of the 26 data sets converge when the initial value for the coefficients are on the limits for the intervals and they all gives results similar to the results in table 3.9 and table 3.10.

	Iv No.	$\sum \lvert\Delta res\rvert$	$\max \lvert\Delta res\rvert$	$\lvert\Delta coe\rvert$	$\#it$
`m824cs.m`					
	2	1.1160	$3.8963 \cdot 10^{-2}$	[0.0006 0.0005 0.0005 ... 0.0009 0.0109 0.0468 0.0420 ... 0.1868 0.1904 0.0789 0.0778]	773
	3	1.3963	$7.3816 \cdot 10^{-2}$	$10^{-1} \cdot$ [0.0030 0.0025 0.0046 ... 0.0052 0.2100 0.3840 0.2960 ... 0.8982 0.9185 0.5243 0.5171]	507
	4	1.4851	$7.2301 \cdot 10^{-2}$	$10^{-1} \cdot$ [0.0011 0.0012 0.0008 ... 0.0016 0.1950 0.0994 0.1735 ... 0.2742 0.2762 0.1401 0.1389]	455
	5	1.1839	$3.9073 \cdot 10^{-2}$	[0.0007 0.0006 0.0004 ... 0.0013 0.0101 0.0366 0.0321 ... 0.2221 0.2263 0.1108 0.1094]	773
	6	0.6186	$7.5054 \cdot 10^{-3}$	$10^{-1} \cdot$ [0.0017 0.0016 0.0001 ... 0.0036 0.0056 0.0427 0.0447 ... 0.4733 0.4821 0.3512 0.3467]	710
	7	1.5577	$6.7282 \cdot 10^{-2}$	[0.0003 0.0003 0.0003 ... 0.0015 0.0155 0.0098 0.0024 ... 0.0995 0.1018 0.1308 0.1291]	474
	8	0.3853	$1.4567 \cdot 10^{-2}$	$10^{-1} \cdot$ [0.0009 0.0009 0.0015 ... 0.0034 0.0442 0.1993 0.1805 ... 0.2391 0.2430 0.3507 0.3465]	535
	9	0.6450	$2.3401 \cdot 10^{-2}$	$10^{-1} \cdot$ [0.0028 0.0026 0.0005 ... 0.0067 0.0554 0.2334 0.2533 ... 0.8297 0.8459 0.6268 0.6187]	546

Table 3.9: Results of the test of the initial value in the new product model. Reference initial value No. 1 = [0.004 0.008 0.002 0.004 0.008 0.9 0.1 0.9 0.1 0.9 0.1].

It can be seen that all the values of $\max |\Delta res|$ in the tables are almost in the order of 10^{-2} or less and all values of $\sum |\Delta res|$ are much smaller than the worst case limit on 15. This is also the case for the other data sets which converge. The data sets which does not converge are the same data sets which did not converge in the test for the perturbation in the new product model and it is therefore assumed that these data sets are not good to use with the new product model because of the irregularities. This means that all converging data sets give good results if the initial values for the coefficients are inside the intervals.

	Iv No.	$\sum \lvert \Delta res \rvert$	$\max \lvert \Delta res \rvert$	$\lvert \Delta coe \rvert$	$\#it$
`m824rd.m`					
	2	1.7559	$4.6047 \cdot 10^{-2}$	[0.0042 0.0045 0.0001 ... 0.0005 0.0001 0.0257 0.0275 ... 0.3077 0.3113 0.1305 0.1345]	361
	3	1.9094	$1.4553 \cdot 10^{-2}$	$10^{-2} \cdot$ [0.0047 0.0041 0.0002 ... 0.0014 0.0120 0.0181 0.0104 ... 0.4859 0.4990 0.3399 0.3486]	313
	4	0.0926	$2.0752 \cdot 10^{-3}$	$10^{-2} \cdot$ [0.0028 0.0029 0.0003 ... 0.0005 0.0310 0.0067 0.0615 ... 0.3676 0.3723 0.1062 0.1107]	326
	5	0.0534	$1.2922 \cdot 10^{-3}$	$10^{-3} \cdot$ [0.0021 0.0062 0.0016 ... 0.0001 0.2054 0.2095 0.1649 ... 0.2279 0.2287 0.0079 0.0033]	323
	6	0.5220	$4.4774 \cdot 10^{-3}$	$10^{-3} \cdot$ [0.0039 0.0268 0.0027 ... 0.0022 0.5227 0.7416 0.1684 ... 0.8424 0.8557 0.2238 0.2664]	341
	7	1.9665	$1.6729 \cdot 10^{-2}$	$10^{-2} \cdot$ [0.0019 0.0079 0.0003 ... 0.0032 0.1409 0.0366 0.1517 ... 0.1498 0.1479 0.4890 0.5354]	301
	8	0.1422	$2.0916 \cdot 10^{-3}$	$10^{-1} \cdot$ [0.0008 0.0009 0.0003 ... 0.0004 0.0039 0.1081 0.0913 ... 0.0981 0.0993 0.1001 0.1034]	318
	9	0.1267	$1.1592 \cdot 10^{-3}$	$10^{-1} \cdot$ [0.0008 0.0009 0.0003 ... 0.0004 0.0018 0.1060 0.0932 ... 0.0982 0.0994 0.1001 0.1033]	326

Table 3.10: Results of the test of the initial value in the new product model. Reference initial value No. 1 = [0.004 0.008 0.002 0.004 0.008 0.9 0.1 0.9 0.1 0.9 0.1].

3.8 Test of the first steps both models

Both models are initiated by setting the first calculated product temperature T_p and container temperature T_c equal to the first value of the measured product temperature in the data set. In the `for`-loop in the implementations T_p is calculated first, afterwards T_c is calculated.
As s result the two first T_p's will always be the same. To avoid this, a new implementation is tested by comparing the mean value and the variance of the residue to the same values from the present implementation. This is done for 26 different data sets.

3.8.1 The present product model

All the 26 data sets gives results similar to the results for the data sets `m824cs.m` and `m824rd.m` in table 3.11.
The mean values and the variances for the same data set are almost the same for both implementations. The minimum value of the variances for all the data sets for present

Data set	Present	implementation	New	implementation
	mean	variance	mean	variance
`m824cs.m`	-0.0234	0.4668	-0.0114	0.4891
`m824rd.m`	0.0300	0.5189	0.0374	0.5282

Table 3.11: The mean values and the variances for the present model with the present and the new implementation.

implementation is 0.1541 and the maximum value of the variances for all data sets for present implementation is 0.9790. The minimum value of the variances for all data sets for the new implementation is 0.1600 and the maximum value of the variances for all data sets for new implementation is 0.9835. The minimum values are found for the same data set in both implementations and are almost completely the same and the same holds true for the maximum values. This means that it does not make a difference if the order of the `if`-statements is exchanged.

3.8.2 The new product model

Almost all the 26 data sets, except 2 which does not converge with the present implementation, give results similar to the results for the data sets `m824cs.m` and `m824rd.m` in table 3.12.

Data set	Present	implementation	New	implementation
	mean	variance	mean	variance
`m824cs.m`	-0.0371	0.1670	-0.0638	1.1300
`m824rd.m`	-0.0345	0.2032	-0.0834	1.0718

Table 3.12: The mean values and the variances for the new model with the present and the new implementation.

The mean values for all the converging data sets for the new implementation are further from 0 than the mean values for the present implementation. The variances for all converging data sets for the new implementation are larger than for the present implementation.

The minimum value of the variances for all the data sets for present implementation is 0.0065 and the maximum value of the variances for all data sets for present implementation is 0.2740. The minimum value of the variances for all data sets for the new implementation is 0.0182 and the maximum value of the variances for all data sets for new implementation is 2.8990. The minimum values are found for the same data set in both implementations but this is not the case for the maximum value.

This means that for the new model it makes a large difference if the order of the `if`-statements is exchanged and it is a bad choice to do so.

3.9 Summary

Both models give good results if the perturbation is 0.001 as it was used in the preproject. Intervals for the initial values for all coefficients in both models are found. The first steps in both models are investigated. In the present model it does not make a difference if the order of the `if`-statements is exchanged, but in the new model it gives bad results to exchange the order. In general the variance for the residue in the new model is smaller than the variance for the residue in the present model if the present implementation where the order of the `if`-statements is not exchanged is used. The mean values of the residues for the present implementation are almost the same for both models.
Thereby the new product model gives the best results, but during the tests is was also found that the new model is more sensitive for irregularities in the data sets than the present model is.

Chapter 4

Experiments

The experiments are made by letting a container with a thermometer inside be transported through a mini pasteur like the one on figure 2.1. Three different types of containers are used, $33cl$ cans, $75cl$ cans and $25cl$ bottles. There are two types of thermometers, one with only one measuring point at the end of the thermometer and one with 10 measuring points separated with approximately 1 cm, see figure 4.1. Both types of thermometers are connected to a computer which collects the data.

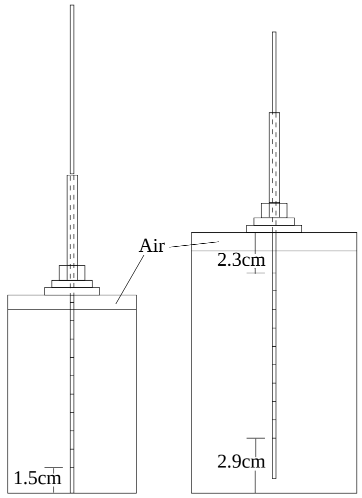

Figure 4.1: Small and large can with the thermometer with 10 measuring points.

To get the thermometer into the cans they are turn up side down and a little hole is made in the center of the bottom. In this hole a threaded bolt with a rubber disk is screwed, se figure 4.4. In the bolt a metal tube is screwed and through this tube the thermometer is placed in the can, se figure 4.2 and figure 4.3. The small can is $10.8cm$ high and $6.4cm$ wide. The large can is $14.2cm$ high and $8cm$ wide.

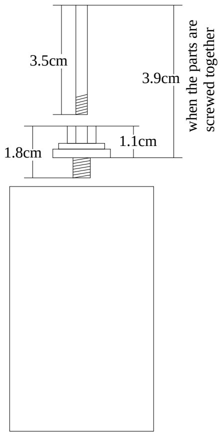

Figure 4.2: Experimental set-up for the can.

Figure 4.3: Experimental set-up for the can.

Figure 4.4: The threaded bolt with rubber disk and metal tube.

To get the thermometer into the bottles they are opened and a plastic stopper with a small hole in the center is glued on. In the hole the thermometer is placed, se figure 4.5 and figure 4.6. The bottle is 18.5cm high and 5.6cm wide.

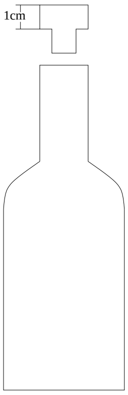

Figure 4.5: Experimental set-up for the bottle.

Figure 4.6: Experimental set-up for the bottle.

When the thermometer is placed in the container, the container is placed on the belt conveyor in the mini pasteur and the cables from the thermometer is arranged so they do not interfere with the experimental set-up, se figure 4.7.
Then the belt conveyor is started and the containers are transported into the first zone. When the containers are in the middle of the first zone the belt conveyor is stopped. This

Figure 4.7: Experimental set-up in mini pasteur.

is done because the zones in the mini pasteur are not as wide as in a real pasteur. When the containers have been in the first zone for a decided time they are transported to zone 2, here they are stopped again and in this way the containers are transported through all 5 zones. The results from the experiments with the thermometer with 10 measuring points are described in chapter 5. The results from the experiments with the thermometer with 1 measuring point are described in chapter 6 and chapter 7.

Chapter 5

Results from thermometer with 10 measuring points

Experiments with the thermometer with 10 measuring points are made with the 33*cl* beer can, the 75*cl* beer can and the 25*cl* beer bottle. An experiment where the large can is filled with water is also made.

5.1 Results for the small can

The product temperatures for the small can in the points in figure 4.1 are shown on figure 5.1.

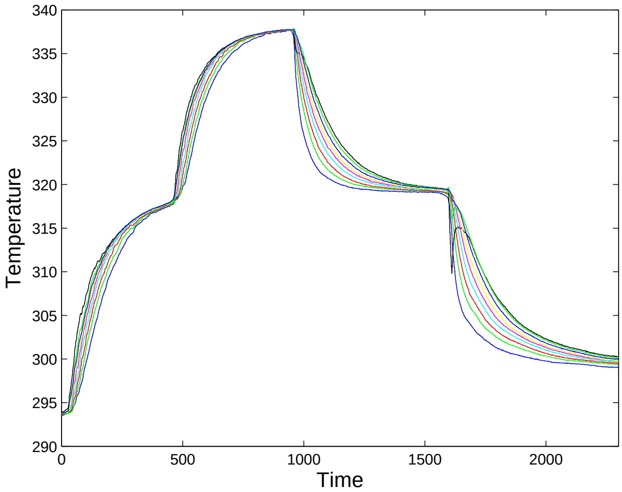

Figure 5.1: Product temperatures as function of time measured with the 10 point thermometer in the small can.

The temperatures are only plotted for the nine lowest measuring points because in the small can the top measuring point is often in the air at the top of the can. The results are not plotted for the first zone because this zone is used to get the product temperature at a certain level. This means that the first zone on the figures really is zone 2 but is referred to as zone 1 because it looks like the first zone on the figures. The lowest blue graph corresponds to the lowest measuring point in the can and the top black graph is the ninth point numbered from the bottom. On figure 5.2 to figure 5.5 there is zoomed in on zone 1, zone 2, zone 3 and zone 4 respectively.

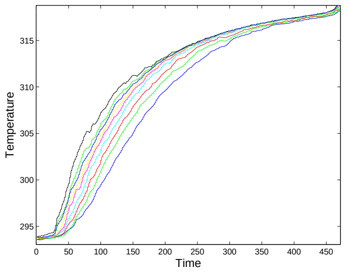

Figure 5.2: Temperatures as function of time zoomed in on zone 1 in the small can.

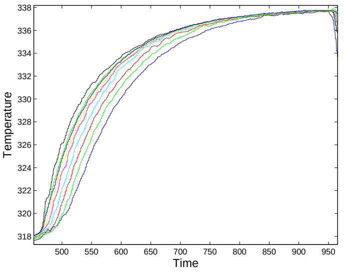

Figure 5.3: Temperatures as function of time zoomed in on zone 2 in the small can.

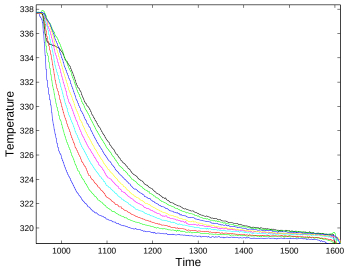

Figure 5.4: Temperatures as function of time zoomed in on zone 3 in the small can.

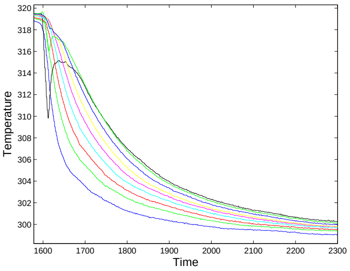

Figure 5.5: Temperatures as function of time zoomed in on zone 4 in the small can.

As it can be seen on figure 5.2 and figure 5.3 the behavior of the product temperatures in the heating zones are very regular. The temperature increases from the top of the can and then down through the product. In the cooling zones on figure 5.4 and figure 5.5 the product temperatures behave more irregular than in the heating zones. On figure 5.6 and figure 5.7 there is zoomed further in on the beginning of zone 3 and zone 4 respectively.

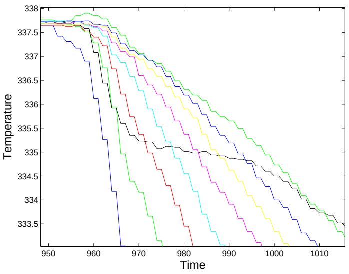

Figure 5.6: Temperatures as function of time zoomed further in on zone 3 in the small can.

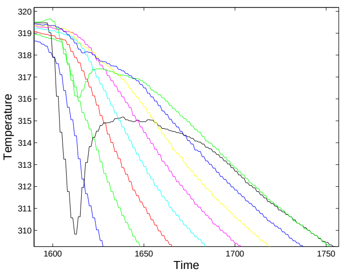

Figure 5.7: Temperatures as function of time zoomed further in on zone 4 in the small can.

At the beginning of zone 3 the highest temperature in the highest point suddenly falls and then after a while the temperature becomes the highest again. In zone 4 the three highest temperatures in three the highest points suddenly falls and then after a while the temperatures become the three highest again.
The reason for these leaps on the graphs is probably a result of the can being mostly affected by the spray water at the top of the can.

5.2 Results for the large can

The product temperatures for the large can in the points on figure 4.1 are shown on figure 5.8.

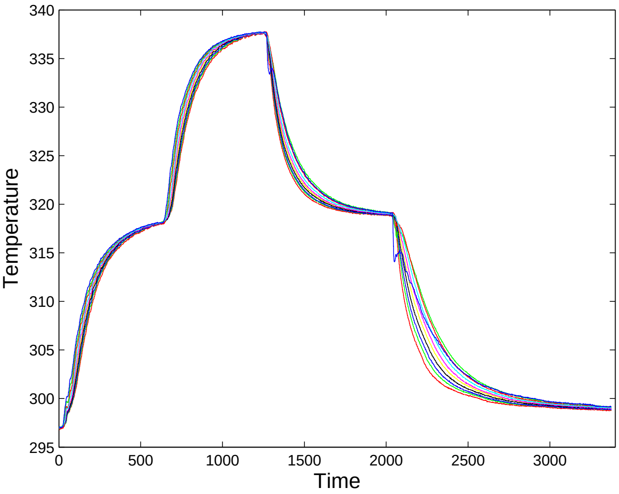

Figure 5.8: Product temperatures as function of time measured with the 10 point thermometer in the large can.

Here the temperature is plotted for all ten measuring points, because in the large can the top measuring point is not in the air at the top of the can. The lowest red graph corresponds to the lowest measuring point in the can and the top blue graph is the top point. On figure 5.9 to figure 5.12 there is zoomed in on zone 1, zone 2, zone 3 and zone 4 respectively.

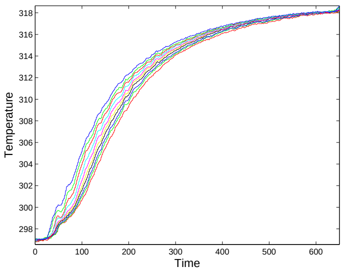

Figure 5.9: Temperatures as function of time zoomed in on zone 1 in the large can.

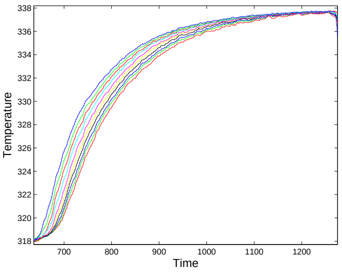

Figure 5.10: Temperatures as function of time zoomed in on zone 2 in the large can.

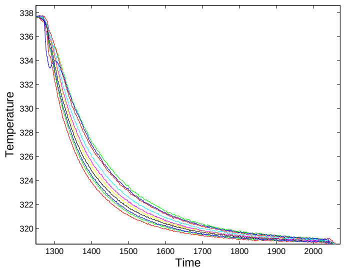

Figure 5.11: Temperatures as function of time zoomed in on zone 3 in the large can.

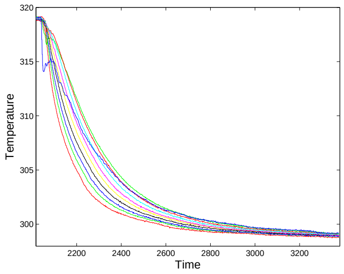

Figure 5.12: Temperatures as function of time zoomed in on zone 4 in the large can.

The product temperature behavior for the large can is similar to the behavior for the small can. The only difference is that the can spends more time in each zone to get the entire product at the same temperature. Further zooming on the two cooling zones can be seen on figure 5.13 and figure 5.14.
The figures for the cooling zones show that the temperatures that makes the leaps in the two cooling zones takes a longer part of the time in the zone to reach the highest temperatures again.

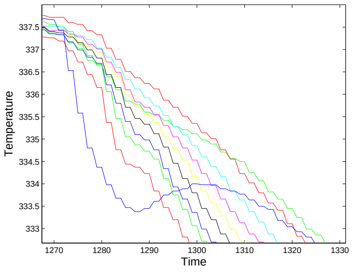

Figure 5.13: Temperatures as function of time zoomed further in on zone 3 in the large can.

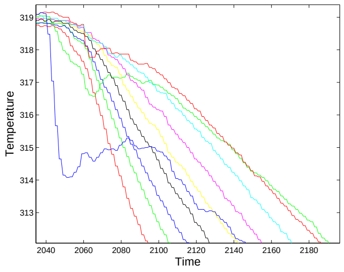

Figure 5.14: Temperatures as function of time zoomed further in on zone 4 in the large can.

5.3 Results for the bottle

The product temperature for the bottle is shown on figure 5.15.

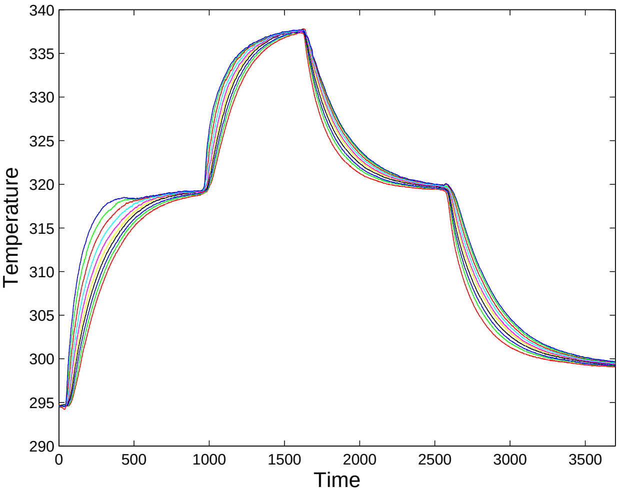

Figure 5.15: Product temperatures as function of time measured with the 10 point thermometer in the bottle.

The temperature is plotted for all ten measuring points. The lowest red graph corresponds to the lowest measuring point in the bottle and the top blue graph is the top point. On figure 5.16 to figure 5.19 there is zoomed in on zone 1, zone 2, zone 3 and zone 4 respectively.

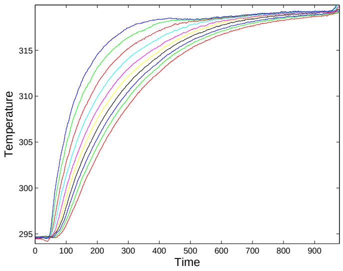

Figure 5.16: Temperatures as function of time zoomed in on zone 1 in the bottle.

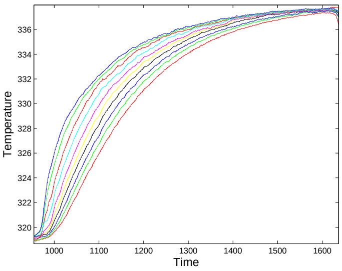

Figure 5.17: Temperatures as function of time zoomed in on zone 2 in the bottle.

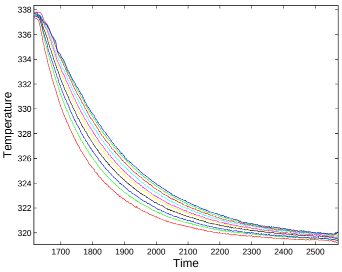

Figure 5.18: Temperatures as function of time zoomed in on zone 3 in the bottle.

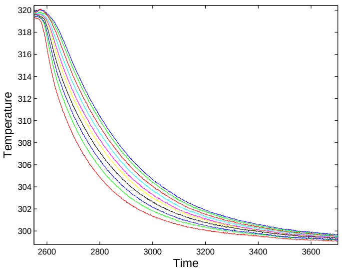

Figure 5.19: Temperatures as function of time zoomed in on zone 4 in the bottle.

The product temperatures for the bottle for all four zones behave regular. The small fall for the highest temperature in zone 1 on figure 5.16 is due to a fall in the spray temperature in the zone during the experiment. The temperatures behave regular also in the cooling zones because the bottle is higher than the cans and is made of glass. The glass bottle is heated slower than the metal cans so the product is not immediately affected by the spray temperature.

5.4 Results for the large can with water

The product temperature for the large can with water is shown on figure 5.20.

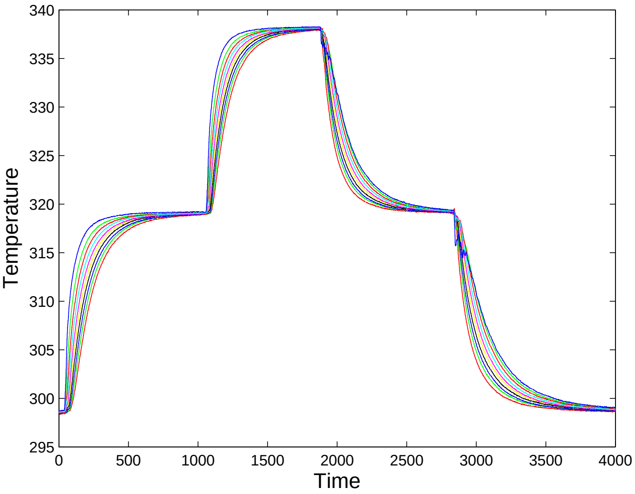

Figure 5.20: Product temperatures as function of time measured with the 10 point thermometer in the large can with water.

The temperature is plotted for all ten measuring points. The lowest red graph corresponds to the lowest measuring point in the can and the top blue graph is the top point. On figure 5.21 to figure 5.24 there is zoomed in on zone 1, zone 2, zone 3 and zone 4 respectively.

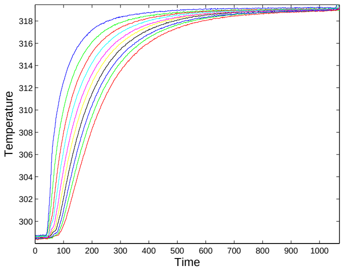

Figure 5.21: Temperatures as function of time zoomed in on zone 1 in the large can with water.

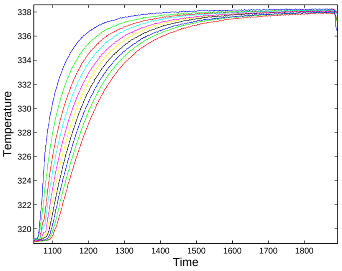

Figure 5.22: Temperatures as function of time zoomed in on zone 2 in the large can with water.

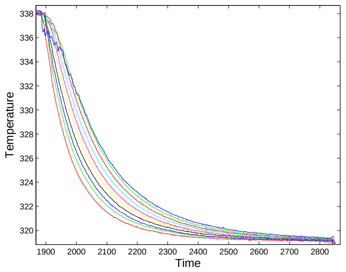

Figure 5.23: Temperatures as function of time zoomed in on zone 3 in the large can with water.

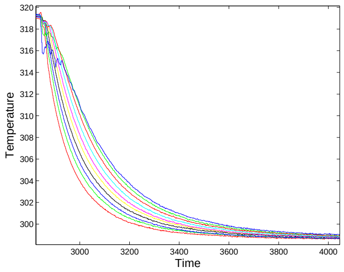

Figure 5.24: Temperatures as function of time zoomed in on zone 4 in the large can with water.

The product temperature behavior for the large can with water is similar to the behavior for the large can with beer. The difference is that the temperature in the top of the can with water increases faster than the temperature in the top of the large can with beer. The temperature down through the can with water is more scattered than the temperature in the large can with beer. The last difference means that it takes longer time for the can with water to get the same temperature down through the can than it takes for the same can with beer. Further zooming on the two cooling zones can be seen on figure 5.25 and figure 5.26.

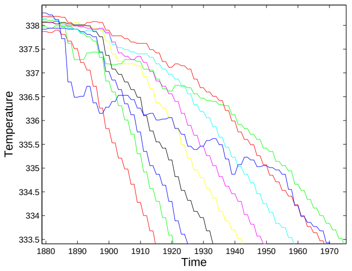

Figure 5.25: Temperatures as function of time zoomed further in on zone 3 in the large can with water.

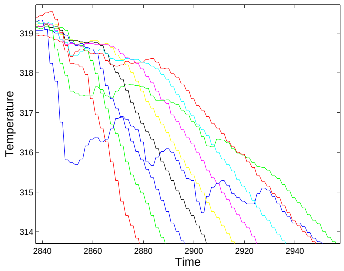

Figure 5.26: Temperatures as function of time zoomed further in on zone 4 in the large can with water.

These figures show that the temperature for the can with water makes approximately the same leaps in the two cooling zones as the leaps on the graph for the large can with beer.

Chapter 6

Investigation of the temperature in the gaps

In the preproject a new spray temperature in the gaps was tested. This new spray temperature in the gaps did not give better results for the present product model. The results for the new product model were better but the largest variation of the residue was still by the gaps.

6.1 Gap temperature

To investigate if the residue in the gaps can be of the same size as in the spray zones the actual spray temperature in the gaps is examined.
To test how the actual spray temperature in the gaps is, some experiments are made. The experiments are made by placing the thermometer with 1 measuring point in a plastic cup with many small holes in the bottom. In this way the thermometer is in water in the spray zones because more spray water comes into the cup than out and the thermometer is in air when the cup is transported into the gap because the water runs quickly out when no more water comes in. This means that the thermometer will measure the spray temperature that the containers goes through while it is transported through the mini pasteur. On figure 6.1 the present modelled spray temperature `spray` and two with thermometer in a cup measured spray temperature is shown.

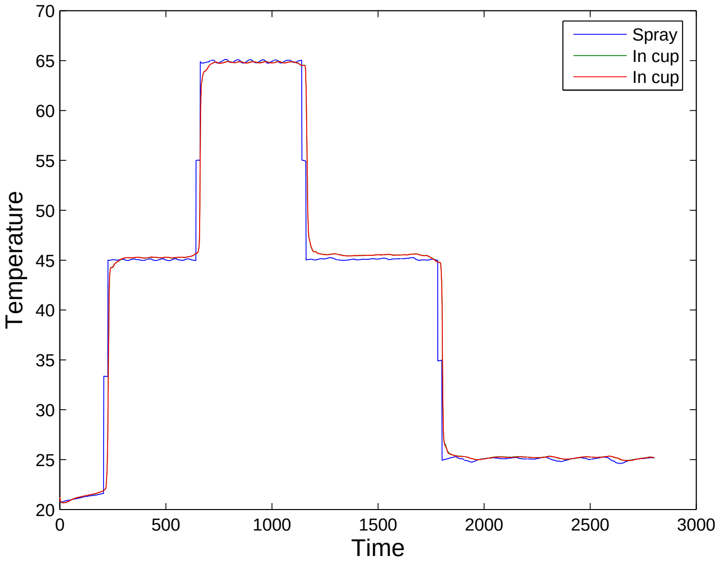

Figure 6.1: Modelled and measured spray temperature.

As it can be seen the measured spray temperature coincide with the modelled spray temperature in the spray zones, but in the gaps there is a difference. Figure 6.2 to figure 6.5 shows the same as figure 6.1 but zoomed in on each gap.

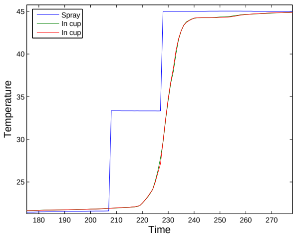

Figure 6.2: Modelled and measured spray temperature, zoomed in on the first gap.

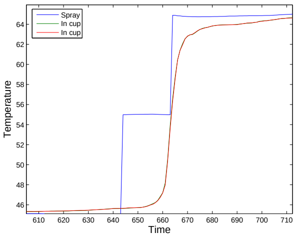

Figure 6.3: Modelled and measured spray temperature, zoomed in on the second gap.

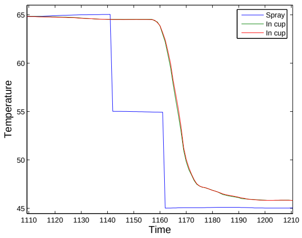

Figure 6.4: Modelled and measured spray temperature, zoomed in on the third gap.

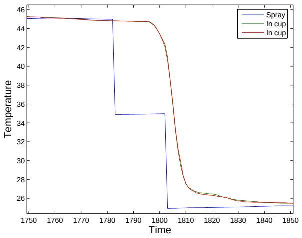

Figure 6.5: Modelled and measured spray temperature, zoomed in on the fourth gap.

To model this the function

$$T_{s,gap}(t) = A + B \tanh\left(\frac{t-b}{a}\right) - C \cdot t \tag{6.1}$$

is used, where $A - B$ is the spray temperature in the previous zone, $A + B$ is the spray temperature in the next zone, $a = 4$ if the next zone is warmer than the previous and $a = -4$ if the next zone is colder than the previous, $C = 0.02$ if the next zone is warmer than the previous and $C = -0.02$ if the next zone is colder than the previous. b is the length of the time the container is in the gap. Function (6.1) is in MATLAB implemented like

```
k=1;
for h=1:length(time)
    if gab(h)==0
       gaplength=0;
    end
    if gab(h)==1
       gaplength=gaplength+1;
    end
    if gab(h)==1 & gab(h+1)==0
       gapL(k)=gaplength;
       k=k+1;
    end
end
gaplength=gapL(1);

figure
plot(time,spraytemp)

for h=1:length(time)
    if gab(h)==1 & gab(h-1)==0
        gaptime=1:gaplength+40;
        Tfor=spraytemp(h-1);
        Tefter=spraytemp(h+gaplength);
        B=abs(Tfor-Tefter)/2-0.5;
        if Tfor>Tefter
            a=-4; b=gaplength; A=Tfor-B; C=-0.02;
        else
            a=4; b=gaplength; A=Tfor+B; C=0.02;
        end
        spraytemp((h):(h)+length(gaptime)-1)=A+B*tanh((gaptime'-b)/a)+C*gaptime';
    end
end
```

The first `for`-loop finds the lengths of the gaps and the second `for`-loop substitutes the present spray temperature in the gaps with the new spray temperature.
With the data set `m824cs.m` where all measurements are used the present and the new spray temperature in the gap can be seen on figure 6.6 to figure 6.9.

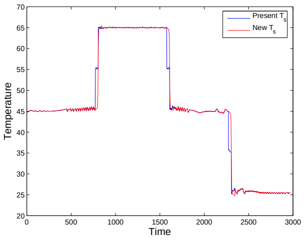

Figure 6.6: Present and new spray temperature.

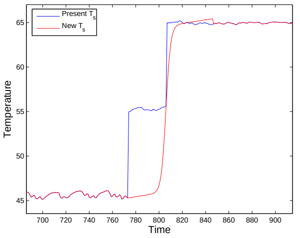

Figure 6.7: Present and new spray temperature, zoomed in on the first gap.

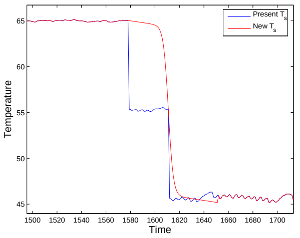

Figure 6.8: Present and new spray temperature, zoomed in on the second gap.

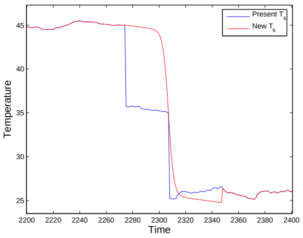

Figure 6.9: Present and new spray temperature, zoomed in on the third gap.

The new spray temperatures in the gaps are very similar to the measured spray temperature in the gaps on figure 6.2 to figure 6.5. 26 data sets are tested with the new spray temperature in the gaps. This is done for both the present product model and the new product model. All the results are made with all measurements from the data sets because if only every tenth were used, the new modelled spray temperature in the gaps would not look like the measured spray temperature in the gaps.

6.1.1 The present product model

With the present product model the mean value and the variance for the two data sets `m824cs.m` and `m824rd.m` are shown for both the present spray temperature in the gaps and the new in table 6.1.

Data set	Present	T_s in gaps	New	T_s in gaps
	mean	variance	mean	variance
`m824cs.m`	-0.0114	0.2339	-0.0161	0.2584
`m824rd.m`	0.0312	0.2582	0.0356	0.2687

Table 6.1: Mean value and variance for the residue for the present model with the present and the new spray temperature in the gaps.

The results in this table are similar to the results for the 24 other data sets which are tested. The new spray temperature in the gaps does not give better results than the present spray temperature in the gaps. The results are almost the same.

6.1.2 The new product model

With the new product model the mean value and the variance for the two data sets `m824cs.m` and `m824rd.m` are shown for both the present spray temperature in the gaps and the new in table 6.2.

Data set	Present	T_s in gaps	New	T_s in gaps
	mean	variance	mean	variance
`m824cs.m`	-0.0239	0.1705	-0.0255	0.1560
`m824rd.m`	-0.0273	0.1801	-0.0232	0.1943

Table 6.2: Mean value and variance for the residue for the new model with the present and the new spray temperature in the gaps.

The results in this table are similar to the results for the 18 other data sets which converged for spray temperatures in the gaps. The results are almost the same so the new spray temperature in the gap does not give better results than the present spray temperature in the gaps.

6.2 Summary

For both product models the results for the present spray temperature in the gaps and the new spray temperature in the gaps are almost the same. The reason for this is that in the experiments in the mini pasteur the containers are in the gaps for a very small part of the total time, only approximately 3% of the time. In the real pasteurs the containers are in the gaps $5 - 10\%$ of the time, so there it might give better results with the new spray temperature in the gaps.

Chapter 7

Coefficients dependency on T and ΔT

To investigate the coefficients from the product models dependency on the spray temperature level T_s and the difference between spray temperatures in two neighboring zones ΔT some experiments are made. The experiments are made with the thermometer with 1 measuring point. In all of them $\Delta T_1 = \Delta T_4$ and $\Delta T_2 = \Delta T_3$, see figure 7.1. Two types of experiments are made, one where the difference in the spray temperatures are the same on both the high and the low T_s level, $\Delta T_1 = \Delta T_2$. This is done for several different values ΔT. These experiments are made to test if the coefficients has a dependency on the spray temperature level. The other experiments are made with different ΔT's on the high and the low T_s level, $\Delta T_1 \neq \Delta T_2$. These experiments are made to test if the coefficients depends on ΔT.

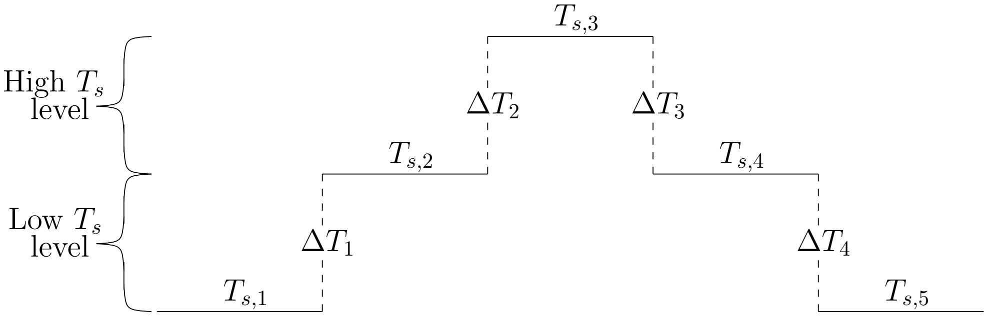

Figure 7.1: Temperatures for the experiments.

The temperatures for the experiments that are made are shown in table 7.1.

Exp. No.	ΔT_1	ΔT_2	ΔT_3	ΔT_4	$T_{s,1}$	$T_{s,2}$	$T_{s,3}$	$T_{s,4}$	$T_{s,5}$
1	15	15	15	15	25	40	55	40	25
2	20	20	20	20	20	40	60	40	20
3	25	25	25	25	15	40	65	40	15
4	10	30	30	10	20	30	60	30	20
5	30	10	10	30	20	50	60	50	20
6	15	35	35	15	15	30	65	30	15
7	35	15	15	35	15	50	65	50	15

Table 7.1: Temperature values for the experiments measured in ℃.

Experiment $1-3$ is to test the coefficients dependency on the spray temperature level and experiment $4-7$ is to test the coefficients dependency on ΔT. To avoid influence from the other coefficients each data set is divided into smaller data sets where each spray zone is in its own data set. In this way the heating coefficients and the cooling coefficients are separated. In experiment 6 it was not possible to keep ΔT_2 and ΔT_3 on 35℃. The difference between spray temperatures were approximately 31℃ , so the results from this experiment are for $\Delta T = 31$ in these zones.

7.1 Present product model

There are 5 coefficients in the present product model, $coe = [c_1\ c_2\ c_3\ c_4\ c_5]$. c_1 is the heating coefficient for the container temperature. c_2 is the heating coefficient for the product temperature. c_3 is the gap coefficient. c_4 is the cooling coefficient for the container temperature. c_5 is the cooling coefficient for the product temperature.
The new small data sets are tested with the present model. In the two heating zones the model gives nice results and the residues are very small. c_1 as function of ΔT can be seen on figure 7.2 and c_2 as function of ΔT is shown on figure 7.3.

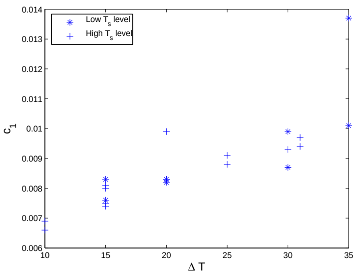

Figure 7.2: c_1 as function of ΔT.

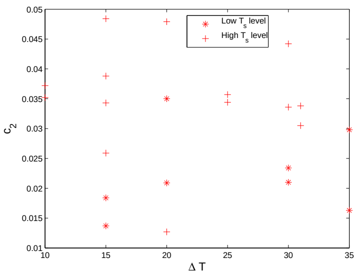

Figure 7.3: c_2 as function of ΔT.

On figure 7.2 the points for the high and the low spray temperature level are not separated, so c_1 does not have a dependency on the spray temperature level however the figure shows that c_1 has a linear dependency on ΔT with a positive slope. On figure 7.3 there is a tendency that shows that the value of c_2 for the high spray temperature level is larger than for the low spray temperature level. This means that c_2 has a dependency on the T_s level and should be found separately in each zone. The figure shows no dependency on ΔT.

The product model for the heating becomes

$$\begin{aligned} T_{c,heat}(t_n) &= T_{c,heat}(t_{n-1}, T_s, c_1(\Delta T), dt) \\ T_{p,heat}(t_n) &= T_{p,heat}(t_{n-1}, T_c, c_2(T_{s-level}), dt) \quad , \end{aligned} \tag{7.1}$$

where $c_1(\Delta T) = A \cdot \Delta T + B$ and $c_2(T_{s-level})$ is constant in each zone, but different from zone to zone.

In the two cooling zones the model does not coincide very well with the measured product temperature so the residue is fairly high. Therefore these data sets are inappropriate and can not be used to test the cooling coefficients.

7.2 New product model

There are 11 coefficients in the new product model, $coe = [c_1\ c_2\ c_3\ c_4\ c_5\ c_6\ c_7\ c_8\ c_9\ c_{10}\ c_{11}]$. c_1 to c_5 are equivalent to the coefficients in the present product model. c_6 and c_7 are the weights of the spray temperature and the product temperature respectively for the container temperature in the gap. c_8 and c_9 are the weights of the spray temperature and the product temperature respectively for the container temperature during heating. c_{10} and c_{11} are the weights of the spray temperature and the product temperature respectively for the container temperature during cooling.

The new product model also gives nice results in the two heating zones. c_1 as function of ΔT is shown on figure 7.4 and c_2 as function of ΔT can be seen on figure 7.5.

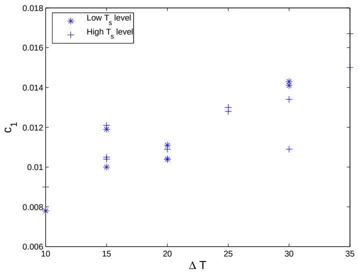

Figure 7.4: c_1 as function of ΔT.

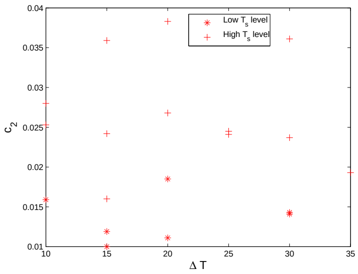

Figure 7.5: c_2 as function of ΔT.

The results for c_1 and c_2 for the new product model are similar to the results for c_1 and c_2 for the present product model. c_1 does not depend on the spray temperature level but has a linear dependency on ΔT with a positive slope. c_2 depends on the spray temperature level with the highest values for the high spray temperature level and smaller values for the low spray temperature level. c_2 does not depend on ΔT.

c_8 as function of ΔT can be seen on figure 7.6 and on figure 7.7 c_9 as function of ΔT is shown.

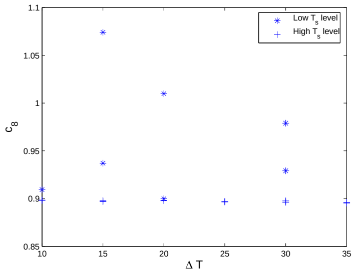

Figure 7.6: c_8 as function of ΔT.

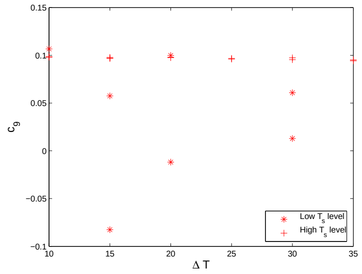

Figure 7.7: c_9 as function of ΔT.

Most of the values of c_8 are approximately 0.9 and the values of c_9 are approximately 0.1 only some single values differ from these values. The values which differs from the almost constant values are all for the low spray temperature level, but some values from the low spray temperature level are also on the constant level, so there is no dependency on the spray temperature level. c_8 and c_9 does not seem to have a dependency on ΔT.
The product model for heating becomes

$$\begin{aligned} T_{c,heat}(t_n) &= T_{c,heat}(t_{n-1}, T_s, T_p, c_1(\Delta T), c_8, c_9, dt) \\ T_{p,heat}(t_n) &= T_{p,heat}(t_{n-1}, T_c, -c_2(T_{s-level})) \ , \end{aligned} \tag{7.2}$$

where $c_1(\Delta T) = A \cdot \Delta T + B$, $c_2(T_{s-level})$ is constant in each zone, but different from zone to zone and c_8 and c_9 are constants.
Again the model does not coincide very well with the measured product temperature in the two cooling zones so these data sets are inappropriate and can also not be used to test the cooling coefficients in the new product model.

Chapter 8

COMSOL modelling

To describe the flow and the temperature in the product during pasteurization the heat transfer equation coupled with the non-isothermal Navier-Stokes equations are investigated.
The expectations to the flow are that it during heating flows up along the side of the container and down in the middle because the product is heated from the side. During cooling it is expected that the flow turns and flows down along the side and up in the middle. Because of this flow it is expected that the temperature increases from the top of the container during heating and that the temperature decreases from the bottom during cooling. These expectations are based on that beer behaves almost like water and when water is above 4℃ and is heated the density decreases.
To the investigation of the flow and temperature the program COMSOL Multiphysics is used. COMSOL uses the finite element method to solve the partial differential equations, [8, p312–319, p328–335, p521].
Normally the finite volume method would be used to solve the Navier-Stokes equations but in this case the velocities in the flow are so small that the finite element method can also be used.

8.1 Partial differential equations

The partial differential equations used to the COMSOL model are the general heat transfer equation coupled with the non-isothermal Navier-Stokes equation, [9, p121–139,p151–166].
The general heat transfer equation through a fluid with both convection and conduction is

$$\delta_{ts}\rho C_p \frac{\partial T}{\partial t} + \nabla\left(-k\nabla T + \rho C_p \boldsymbol{u}\nabla T\right) = Q \quad , \tag{8.1}$$

where T is the temperature, t is the time, δ_{ts} is the time scaling coefficient, k is the thermal conductivity, ρ is the density, C_p is the heat capacity, Q is the heat source and $\boldsymbol{u} = [u\ v]$ is the velocity field, where u is the $r-$velocity and v is the $z-$velocity, [2].
In this case $\delta_{ts} = 1$ as the calculations are made in seconds. $Q = 0$ because the added heat is added through the boundaries. k, ρ and C_p are all functions of the temperature

$k = k(T)$, $\rho = \rho(T)$ and $C_p = C_p(T)$. u and v are calculated in the Navier-Stokes equations.

The non-isothermal Navier-Stokes equations are

$$\rho\left(\boldsymbol{u}\nabla\right)\boldsymbol{u} = \nabla\left(-p\boldsymbol{I} + \eta\left(\nabla\boldsymbol{u} + (\nabla\boldsymbol{u})^T\right) - \left(\frac{2\eta}{3} - \kappa\right)\left(\nabla\boldsymbol{u}\right)\boldsymbol{I}\right) + \boldsymbol{F} \tag{8.2}$$

$$\nabla\left(\rho\boldsymbol{u}\right) = 0 \quad , \tag{8.3}$$

where p is the pressure, η is the dynamic viscosity, κ is the dilatational viscosity and $\boldsymbol{F} = [F_r\ F_z]$ is the volume force, where F_r is the volume force in the $r-$direction and F_z is the volume force in the $z-$direction, [3, ch11,p1–10]. η is a function of the temperature $\eta = \eta(T)$, $\kappa = 0$, $F_r = 0$ and $F_z = 9.81 \cdot (\rho(T_0) - \rho(T))$ which is the gravity force and has effect as a volume force. When ρ increases the gravity force will increase in downward direction.

The initial conditions for the partial differential equations are $T(t_0) = T_0$, $u(t_0) = 0$, $v(t_0) = 0$, $p(t_0) = 0$. The boundary conditions for the heat transfer are different depending on the place on the boundary. On the sides and the top of the container a Dirichlet boundary conditions is used. The boundary condition is a time depending temperature $T = Tb(t)$ which is equivalent to the spray temperature. In the bottom of the container the boundary is insulated and the boundary condition is $-\boldsymbol{n}(-k\nabla T + \rho C_p\boldsymbol{u}T) = 0$ which is a Neumann boundary condition. The bottom is insulated because the container during pasteurization stands on a plastic belt conveyor and this means that the bottom is not very much affected by the surrounding temperature. The boundary conditions for the Navier-Stokes equations on all boundaries are that the fluid's velocity equals the velocity of the boundaries which is 0. This is also called no slip and the boundary condition is $\boldsymbol{u} = \boldsymbol{0}$ which is a Dirichlet boundary condition.

The expressions for $k(T)$, $\rho(T)$, $C_p(T)$ and $\eta(T)$ are found from the values in table 8.1, [10].

$T[K]$	$\rho[\frac{kg}{m^3}]$	$C_p[\frac{J}{kgK}]$	$\eta[Pas]$	$k[\frac{W}{mK}]$
273.15	999.84	4217.6	0.001793	0.5610
283.15	999.70	4192.1	0.001307	0.5800
293.15	998.21	4181.8	0.001002	0.5984
303.15	995.65	4178.4	0.0007977	0.6154
313.15	992.22	4178.5	0.0006532	0.6305
323.15	988.03	4180.6	0.0005470	0.6435
333.15	983.20	4184.3	0.0004665	0.6543
343.15	977.78	4189.5	0.0004040	0.6631
353.15	971.82	4196.3	0.0003544	0.6700
363.15	965.35	4205.0	0.0003145	0.6753
373.15	958.40	4215.9	0.0002188	0.6791

Table 8.1: Values of ρ, C_p, η and k for different values of T.

The values in the table is for water. MATLAB's fitting tools are used to find cubic expressions for each of the variables as function of the temperature. The cubic expressions are

$$\begin{aligned}
\rho(T) &= 1.569 \cdot 10^{-5}T^3 - 0.018774T^2 + 6.7647T + 233.17 \ , && (8.4)\\
C_p(T) &= -1.5227 \cdot 10^{-4}T^3 + 0.16194T^2 - 56.582T + 10691 \ , && (8.5)\\
\eta(T) &= -2.9827 \cdot 10^{-9}T^3 + 3.0756 \cdot 10^{-6}T^2 - 0.0010615T + 0.12302 \ , && (8.6)\\
k(T) &= -6.6628 \cdot 10^{-9}T^3 - 2.9149 \cdot 10^{-6}T^2 + 0.0051701T - 0.49841 \ . && (8.7)
\end{aligned}$$

On figure 8.1 to figure 8.4 the values and the cubic expressions for each variable as functions of the temperature can be seen. The figures also show the residuals for each expression. The residuals for each expression are small compared to the size of the variable so the expressions are fine models for the variables.

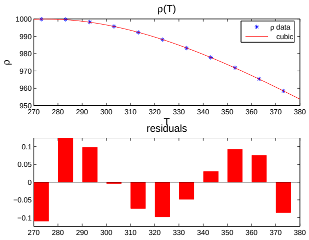

Figure 8.1: ρ as function of T and the residuals.

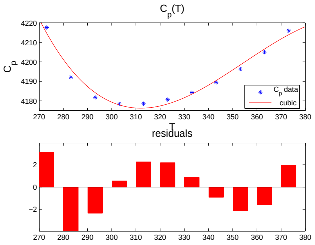

Figure 8.2: C_p as function of T and the residuals.

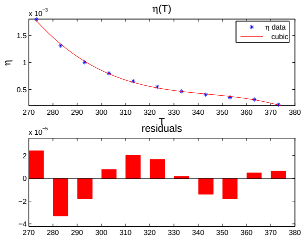

Figure 8.3: η as function of T and the residuals.

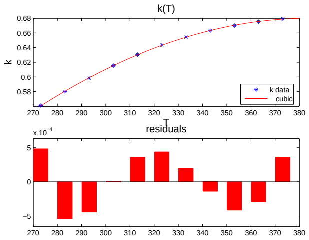

Figure 8.4: k as function of T and the residuals.

8.2 Data entry for making the COMSOL model

Before the actual model in COMSOL is made a `.txt`-file with the boundary temperatures as function of time must be made. The file should look like

```
0    295.0
1    295.004
2    295.00899999999996
3    295.0265
4    295.04999999999995
.      .
.      .
.      .
```

where the times stand to the left and the matching temperatures stands to the right. It is not necessary to have a time and a temperature for all times because the temperatures are interpolated.

Then the model in COMSOL can be made.

Because the containers are cylindrical it is assumed that the geometry of the container is axisymmetric. This means that there are variations in the radial r and the vertical z direction only and not in the angular θ direction.

In the Model Navigator the Space dimension is set to Axial symmetry (2D) and Multiphysics is chosen. Under the Heat Transfer Module the General Heat Transfer (GHT) and the Non-Isothermal Flow (NIF) is added to the same geometry.

Then the container is drawn in Draw Mode. COMSOL works with SI-units so the $r-$ and z-axis are in meters. Because axial symmetry is used only half of the container should be drawn from $r = 0$ to r equal to the width of the container and from $z = 0$ to z equal the height of the container.

Under the Solve menu in the menu bar Solver Parameters is chosen. Here Analysis is set to Transient, the Solver is set to Time dependent and under General in the Time stepping area the output Times are entered as a vector and should be in seconds. The default values are used for the tolerances.

Under the Mesh menu in the menu bar Mesh Parameters is chosen. Here the Predefined mesh sizes is chosen to be empty, Maximum element size is set to 0.008, Maximum element size scaling factor is set to 1, Element growth rate is set to 1.2, Mesh curvature factor is set to 0.3, Mesh curvature cut off is set to 0.001 and Resolution of narrow regions is set to 1. Mesh geometry to level is chosen to Subdomain and Refinement method is chosen to Regular. Then the mesh is made. In the top of the container the mesh should be refined.

Under the Multiphysics menu in the menu bar it is possible to switch between the General Heat Transfer and the Non-Isothermal Flow.

In the Subdomain Settings for the GHT both the conductive and the convective heat transfer are enabled. Under Conduction δ_{ts} is set to 1, k (isotopic) is set to $k(T)$, ρ is set to $rho(T)$, C_p is set to $Cp(T)$ and Q is set to 0. These values are automatically set under Convection so here it is only necessary to set u to u and v to v. Under Init $T(t_0)$ is set to $T0$.

In the Subdomain Settings for the NIF ρ is set to $rho(T)$, η is set to $eta(T)$, κ is set to 0, F_r is set to 0 and F_z is set to $9.81 * (rho(T0) - rho)$. Under Init $u(t_0)$, $v(t_0)$ and $p(t_0)$ are all set to 0.

In the Subdomain Settings for both GHT and NIF it is not necessary to change anything under Element.

In the Boundary Settings for GHT the vertical boundaries at $r = 0$ is set to Axial symmetry, the boundary in the bottom of the container is set to Thermal insulation and the other boundaries on the side and the top of the container is set to Temperature and T_0 is set to $Tb(t)$.
In the Boundary Settings for NIF the vertical boundaries is again set to Axial symmetry. All the other boundaries are set to No slip.
In the Point Settings for NIF the Point constraint is used for the point for r equal to the width of the container and $z = 0$ and p_0 for this point is set to 0. Nothing needs to be changed for the other points.
Under the Options menu in the menu bar Expressions and Scalar Expressions is chosen. Here the name $T0$ is written under Name and the value of $T0$ is written under Expression
Under the Options menu in the menu bar Functions is chosen. A new function with the Function name Tb is made as Interpolation with Use data from File and then finding the `.txt`-file with the boundary temperatures. The Interpolation method should be Linear, the Extrapolation method should be Constant and the Value outside range should be NaN (not a number). New functions with the Function name rho, eta, k and Cp respectively are made for each of the expressions by using Analytic. Then Arguments for all four functions are set to T and Expression is set to the respective expression from the expressions (8.1) to (8.4).
Then the model can be solved by starting the solver.

8.3 Results from COMSOL

Three different models are made in COMSOL, one model with the small can, one model with the large can and one model with a glass ”can”.

8.3.1 Results for the small can

The model for the small can is made with the following data. As the boundary temperature as function of time a measured spray temperature from an experiment saved in the file `tb17a.txt` is used. The initial temperature is $T0 = 295.0$ and the time is $0 \leq t \leq 2300$. The model is solved on the mesh on figure 8.5 and the solution time is approximately $9.5h$ on the DTU system.

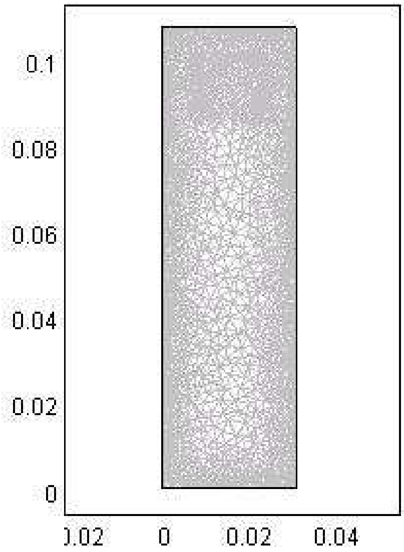

Figure 8.5: The mesh on which the COMSOL model for the small can is solved.

The mesh consist of 4308 elements where as 280 are on the boundaries. The mesh is finer at the boundaries and the top of the can because the heating/cooling affects the product from the boundaries and the interesting phenomena occurs at the top. On figure 8.6 the temperatures as function of time in nine points on the axisymmetric boundary of the small can on figure 4.1 is shown together with the spray temperature from `tb17a.txt` at the point $(0.032, 0.108)$.

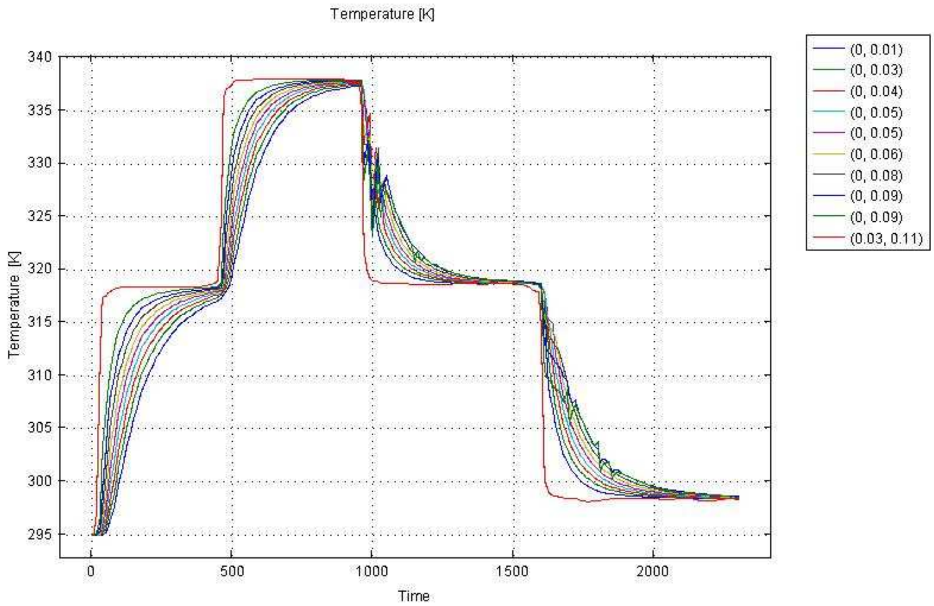

Figure 8.6: Temperatures at $r = 0$ and the spray temperature as functions of time for the small can.

The points on the legend are rounded automatically by COMSOL and should be $(0, 0.015)$, $(0, 0.025)$, $(0, 0.035)$, $(0, 0.045)$, $(0, 0.055)$, $(0, 0.065)$, $(0, 0.075)$, $(0, 0.085)$, $(0, 0.095)$ and $(0.032, 0.108)$. The points at $r = 0$ corresponds to points in the middle of the 3D can. On figure 8.7 and figure 8.8 there is zoomed in on zone 3 and zone 4 respectively, the spray temperature is not plotted on these figures.

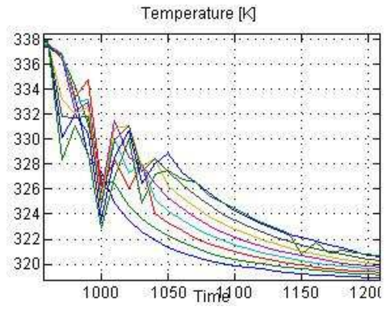

Figure 8.7: Temperatures as function of time zoomed in on zone 3.

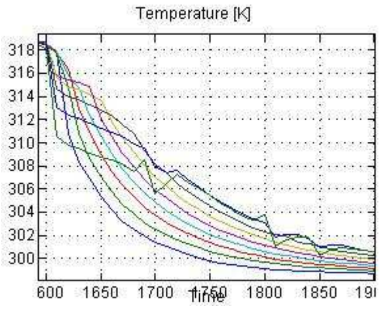

Figure 8.8: Temperatures as function of time zoomed in on zone 4.

As it can be seen the temperatures behave regular during the two first zones which are heating zones. The temperature is highest at the top of the can and decreases down through the can. In the two cooling zones the behavior of the temperatures are irregular. The temperatures make some leaps where some of the temperatures suddenly fall and then gets up again. When the product temperature approaches the spray temperature the highest product temperatures are again at the top of the can and the temperature decreases down through the can.
The product temperatures for the 2D cross section of the half can are plotted for the times $t = 50$, $t = 250$, $t = 470$, $t = 960$, $t = 970$, $t = 980$, $t = 1000$, $t = 1100$, $t = 1610$, $t = 1630$, $t = 1850$ and $t = 2000$ and are shown on figure 8.9 and figure 8.10. Note that the temperature interval for each time is different.

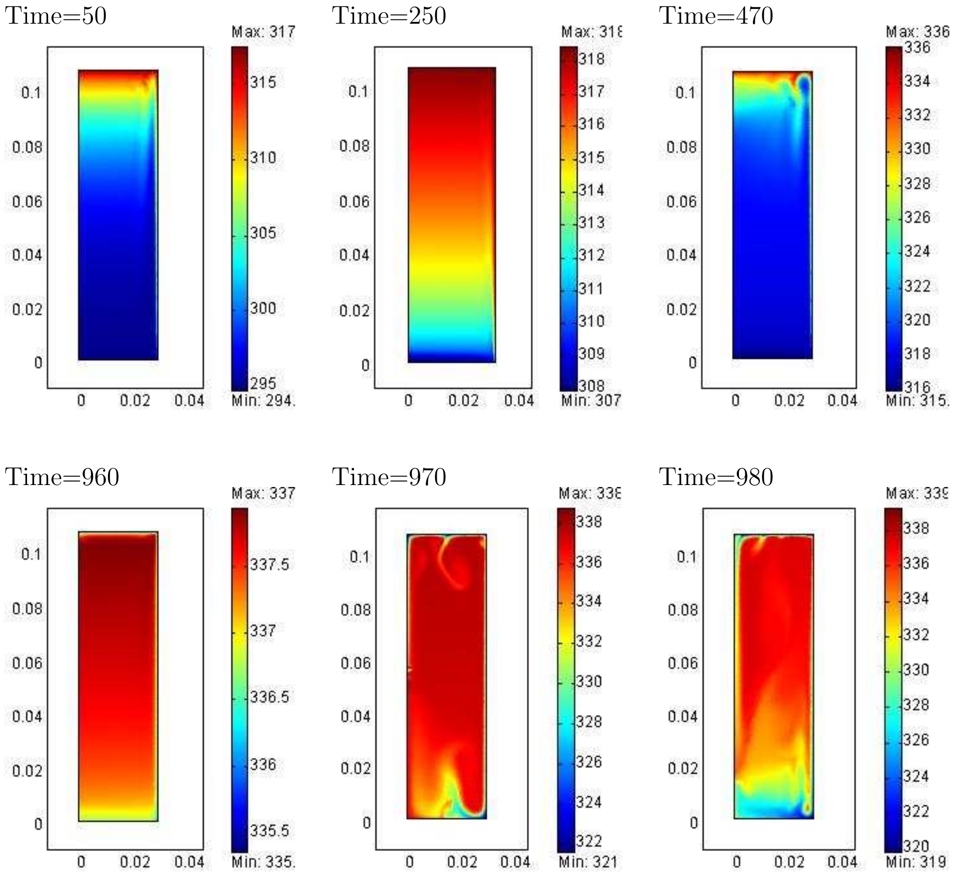

Figure 8.9: Temperatures in the small can for the times $t = 50$, $t = 250$, $t = 470$, $t = 960$, $t = 970$ and $t = 980$. Note that the temperature interval for each time is different.

The two first plots on figure 8.9 for $t = 50$ and $t = 250$ are for the first heating zone and here the temperature increases from the top of the can and down to the bottom. At

$t = 470$ the can has just entered the second zone and here the temperature also increases from the top of the can. At $t = 960$ the can has just entered the third zone which is a cooling zone and at $t = 970$ and $t = 980$ the cooling is started. The temperature decreases from the bottom for the can but much more disordered than the cooling. It looks like the cooled product runs down along the side of the can and then splashes up when it reaches the bottom. At $t = 1000$ there is a cold liquid drop which goes down in the middle of the can almost to the bottom. It is drops like this which is responsible for the leaps on figure 8.6 to figure 8.8. At $t = 1610$ the can has just entered the fourth zone. The behavior in this cooling zone is the same as for zone 3. The only difference is that the drops in the middle of the can do not reach as far to the bottom. There are also liquid drops in the top of the can away from the middle.

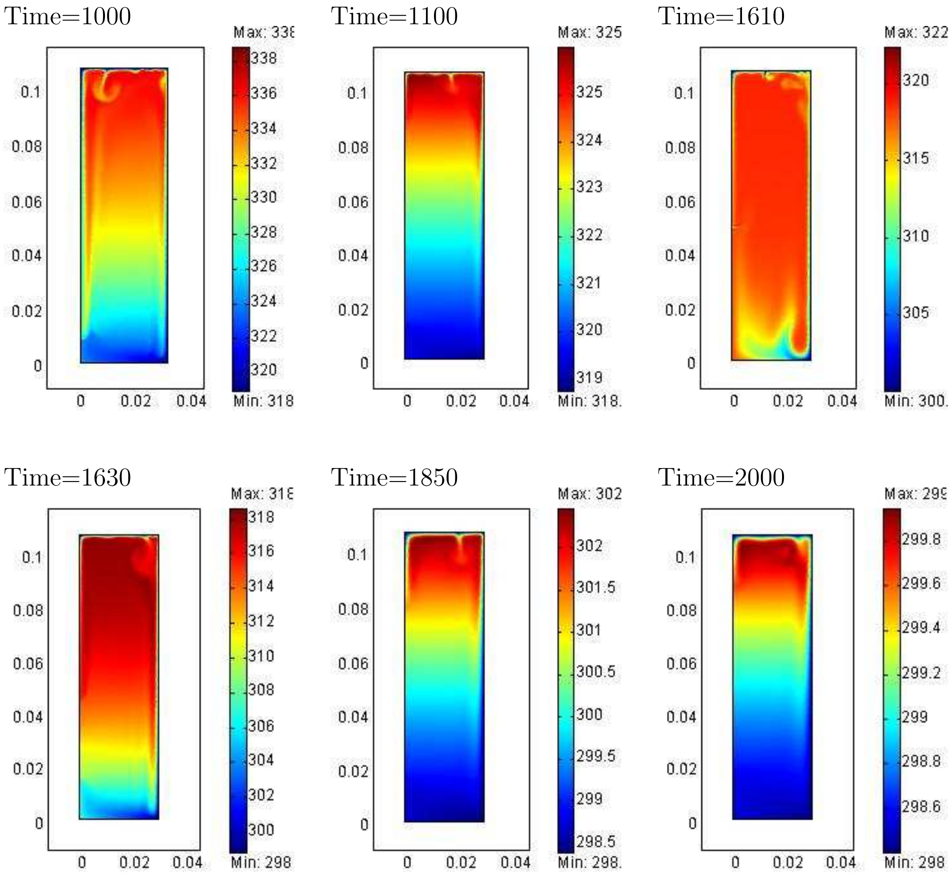

Figure 8.10: Temperatures in the small can for the times $t = 1000$, $t = 1100$, $t = 1610$, $t = 1630$, $t = 1850$ and $t = 2000$. Note that the temperature interval for each time is different.

On figure 8.11 and figure 8.12 the velocity fields are shown with arrows for the same times as the temperatures. All arrows have the same length.

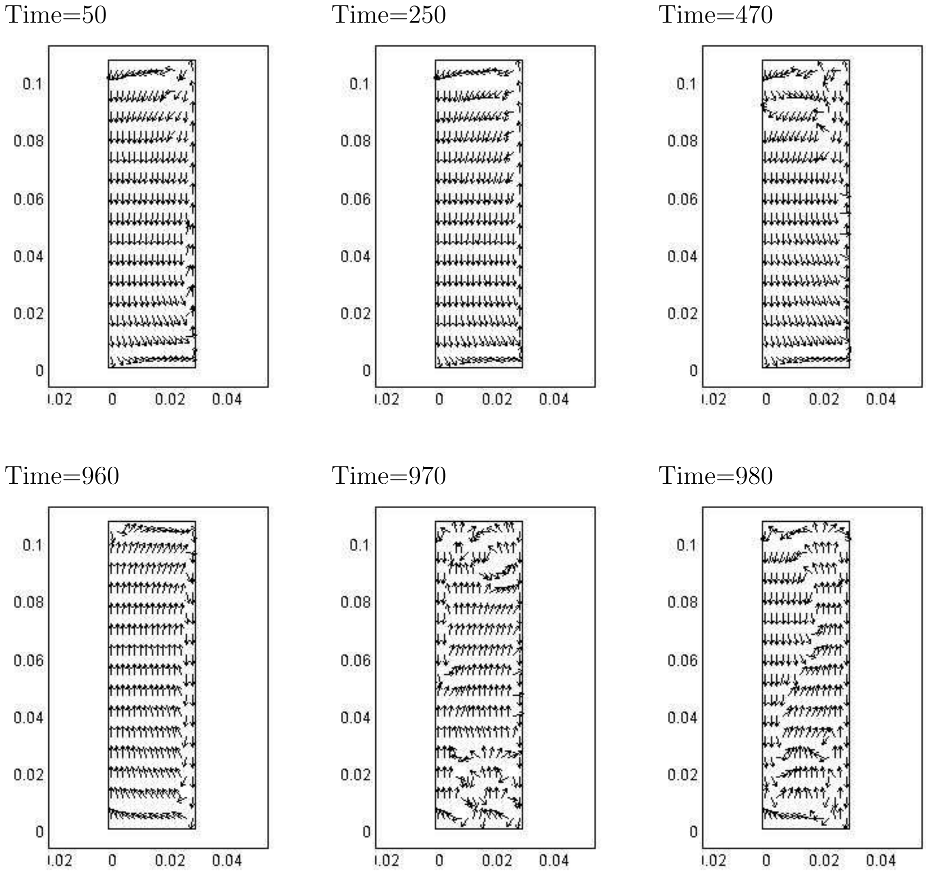

Figure 8.11: Velocity field plotted with arrows in the small can for the times $t = 50$, $t = 250$, $t = 470$, $t = 960$, $t = 970$ and $t = 980$.

At $t = 50$ and $t = 250$ the heating in the first zone is in progress. The velocity field flows up along the side of the can and flows down in the middle. This is as expected because the product is heated from the sides so the product along the sides gets hotter than in the middle and thereby the density gets smaller and the product flows upwards. At $t = 470$ the can has just entered the second zone and a little disorder occurs in the top of the can. This disorder does not affect the temperature very much. At $t = 960$ the cooling is just started. In the beginning of the cooling the velocity field turns around so the cold product along the side of the can flows downwards to the bottom and then forces the hotter product up in the middle. Very quickly the regular flow gets disordered in the top and the bottom of the can where substructures with opposing flow occur and the product starts to flow down in the middle. After a while in the cooling zone at $t = 1100$

the regular flow is back with only small substructures with opposing flow at the top. At $t = 1610$ the can has just entered the fourth zone. The velocity field behaves like in the third zone. The flow gets disordered again and after a while the flow is regular again with only small opposing flows.

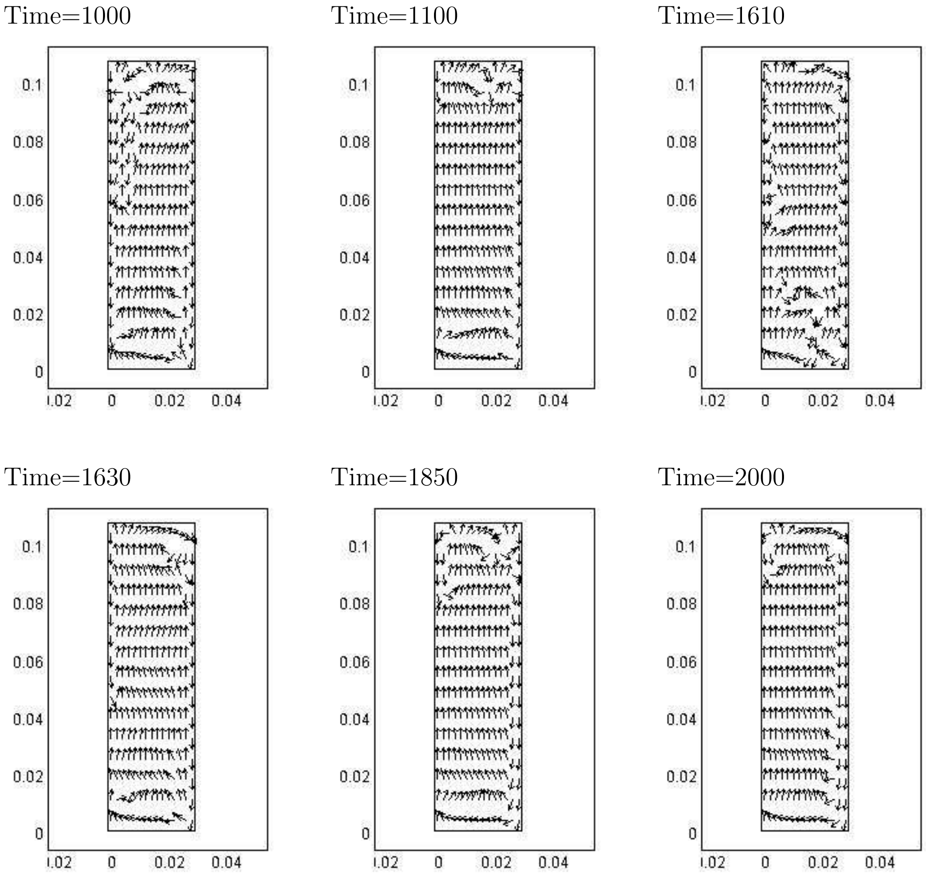

Figure 8.12: Velocity field plotted with arrows in the small can for the times $t = 1000$, $t = 1100$, $t = 1610$, $t = 1630$, $t = 1850$ and $t = 2000$.

On figure 8.13 and figure 8.14 the velocity fields are shown as a contour plot for the same times as the temperatures and the velocity fields with arrows. Note that the velocity interval for each time is different.

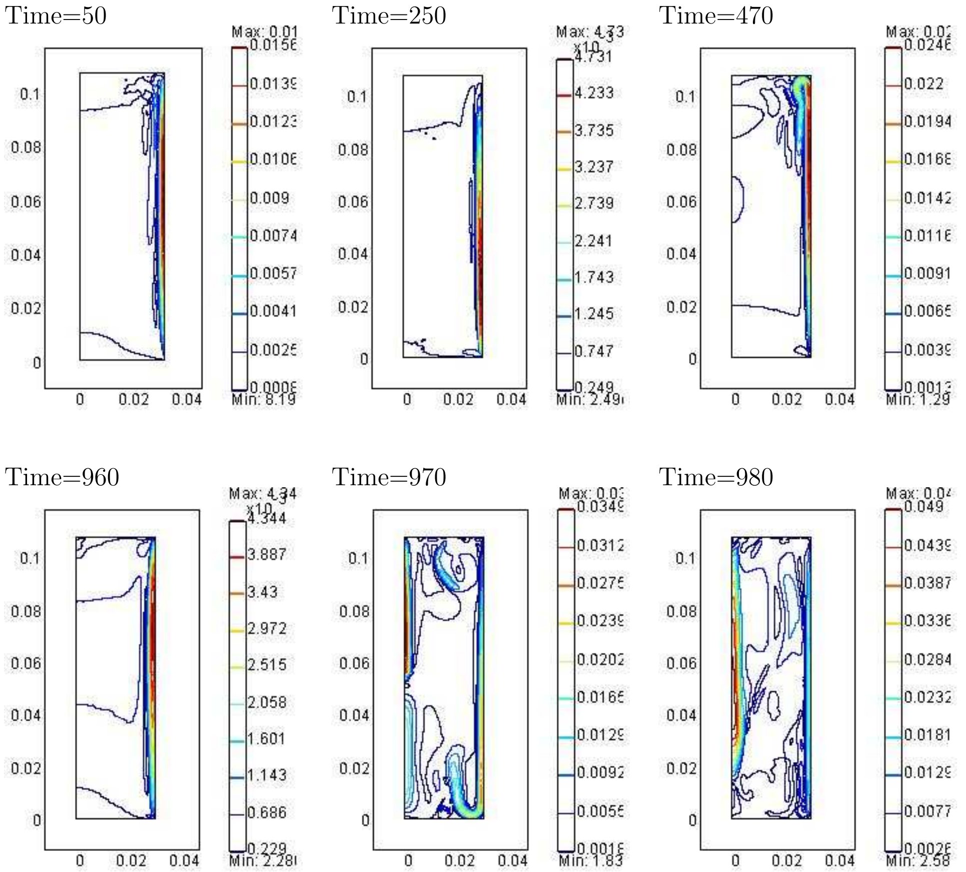

Figure 8.13: Velocity field plotted as contour plot in the small can for the times $t = 50$, $t = 250$, $t = 470$, $t = 960$, $t = 970$ and $t = 980$. Note that the velocity interval for each time is different.

The figures with the contour plots are made to show the order of the velocity field. The largest velocity on the plots is $5.8 \cdot 10^{-2} \frac{m}{s}$. During the heating zones for the times $t = 50$, $t = 250$ and $t = 470$ the velocity is largest near the side of the can. When the disordered substructures with opposing flows occurs in the middle of the can the largest velocity is in these flows and also still near the sides.

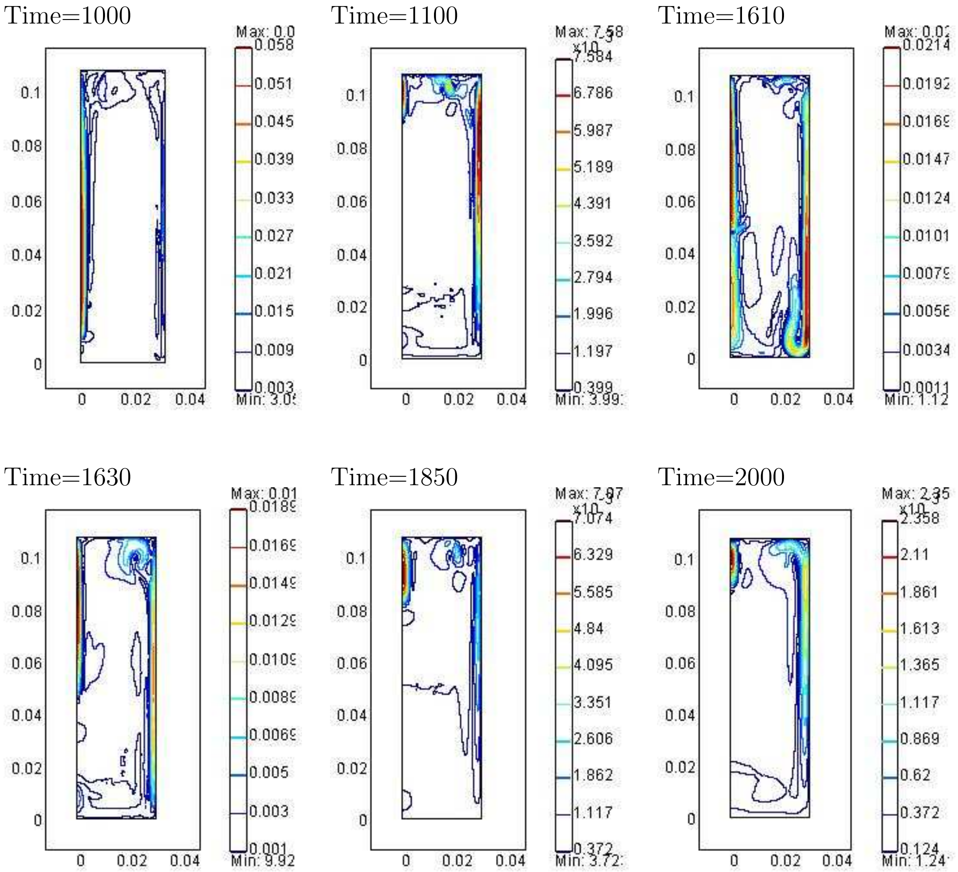

Figure 8.14: Velocity field plotted as contour plot in the small can for the times $t = 1000$, $t = 1100$, $t = 1610$, $t = 1630$, $t = 1850$ and $t = 2000$. Note that the velocity interval for each time is different.

8.3.2 Results for the large can

The model for the large can is made with the following data. As the boundary temperature as function of time a measured spray temperature from an experiment saved in the file `tb19a.txt` is used. The initial temperature is $T0 = 294.6$ and the time is $0 \leq t \leq 3700$. The solution time is approximately $12h$ on the DTU system. The model is solved on the mesh on figure 8.15.

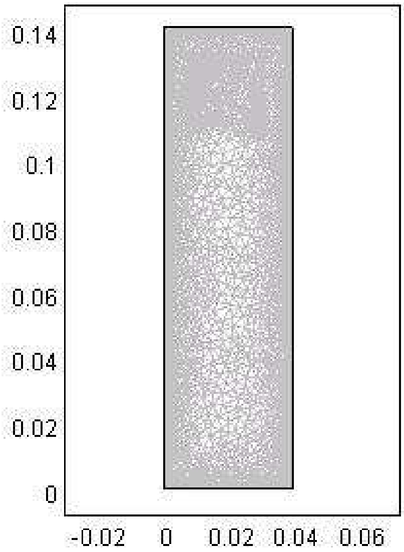

Figure 8.15: The mesh on which the COMSOL model for the large can is solved.

The mesh consist of 6014 elements where as 364 are on the boundaries. On figure 8.16 the temperatures as function of time in the 10 points on the axisymmetric boundary of the large can on figure 4.1 is shown together with the spray temperature from `tb19a.txt` at the point $(0.04, 0.142)$.

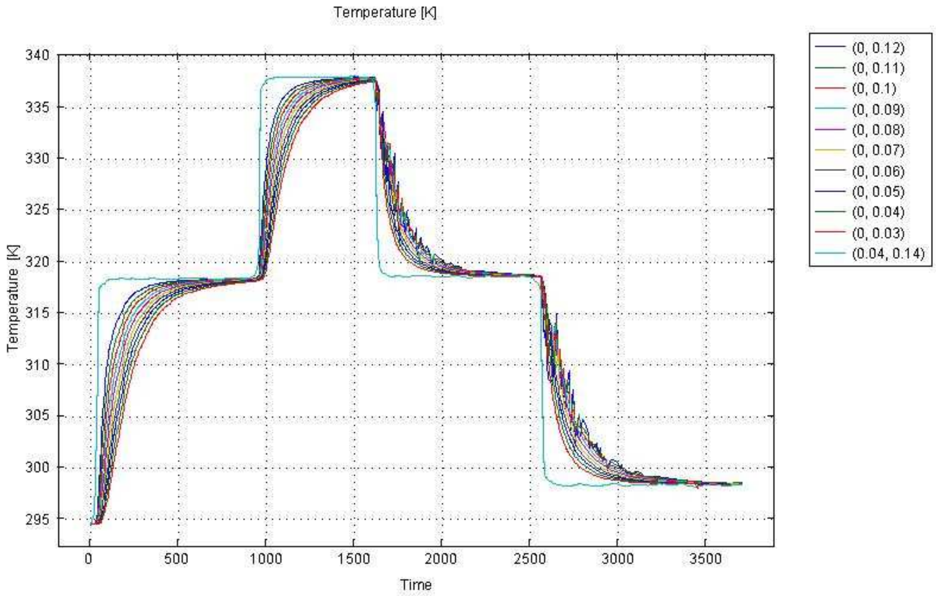

Figure 8.16: Temperatures at $r = 0$ and the spray temperature as functions of time for the large can.

Here the points should be $(0, 0.119)$, $(0, 0.109)$, $(0, 0.099)$, $(0, 0.089)$, $(0, 0.079)$, $(0, 0.069)$, $(0, 0.059)$, $(0, 0.049)$, $(0, 0.039)$, $(0, 0.029)$ and $(0.032, 0.108)$. On figure 8.17 and figure 8.18 there is zoomed in on zone 3 and zone 4 respectively, the spray temperature is not plotted on these figures.

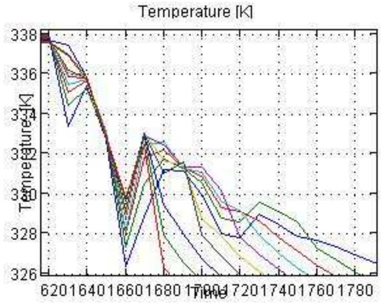

Figure 8.17: Temperatures as function of time zoomed in on zone 3.

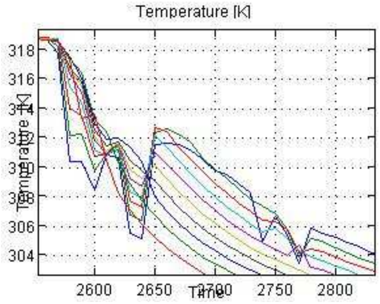

Figure 8.18: Temperatures as function of time zoomed in on zone 4.

As it can be seen on the figures the temperatures in the points in the middle of the large can behave like in the small can. The only difference is that the process is slower for the large can so the timescale is different. The product temperature behavior is regular during the two heating zones and has some leaps after entering the cooling zones. After a while in the cooling zones the behavior of the temperature gets regular again.
The product temperatures for the 2D cross section of the half can are plotted for the times $t = 100$, $t = 600$, $t = 970$, $t = 1620$, $t = 1640$, $t = 1650$, $t = 1730$, $t = 1900$, $t = 2575$, $t = 2590$, $t = 2700$ and $t = 3000$ and are shown on figure 8.19 and figure 8.20. Note that the temperature interval for each time is different.

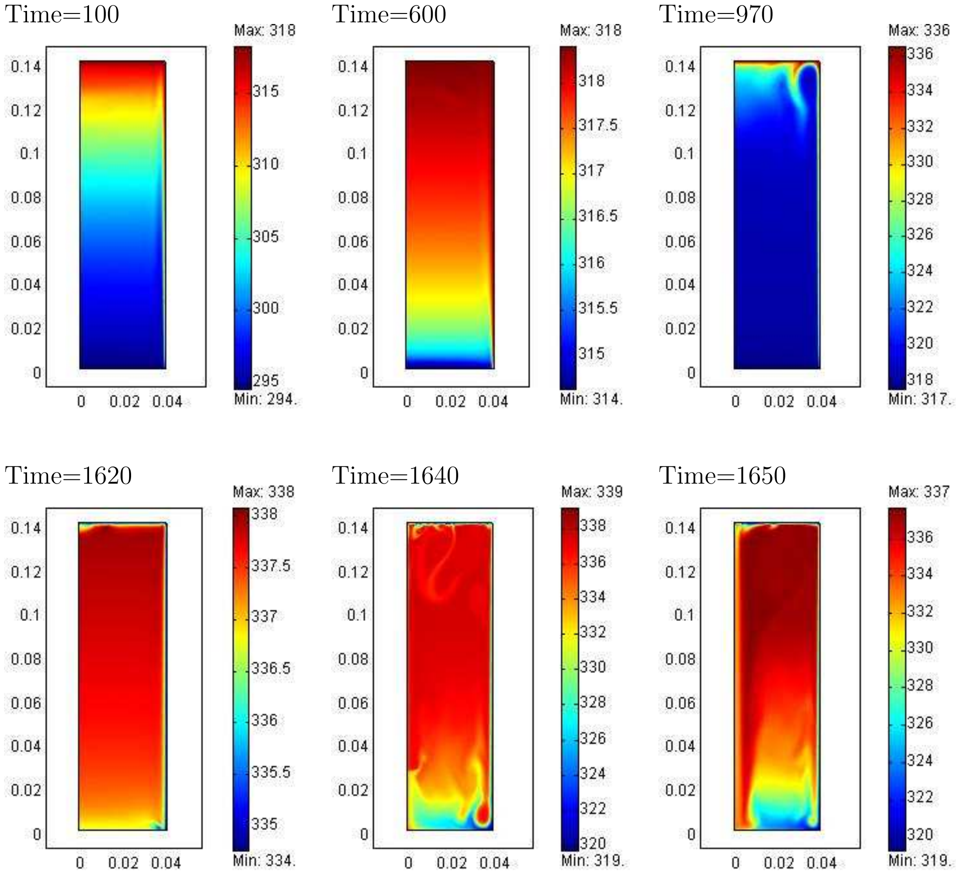
Time=100 Time=600 Time=970

Time=1620 Time=1640 Time=1650

Figure 8.19: Temperatures in the large can for the times $t = 100$, $t = 600$, $t = 970$, $t = 1620$, $t = 1640$ and $t = 1650$. Note that the temperature interval for each time is different.

The times are selected so that the temperature plots correspond to the temperature plots for the small can to show the similarities. The temperatures look very similar to the temperatures in the small can. In the heating zones the temperature increases from the top of the can and down to the bottom. In the cooling zones the temperature decreases from the bottom of the can and to the top. The cooling is more disordered than the heating.

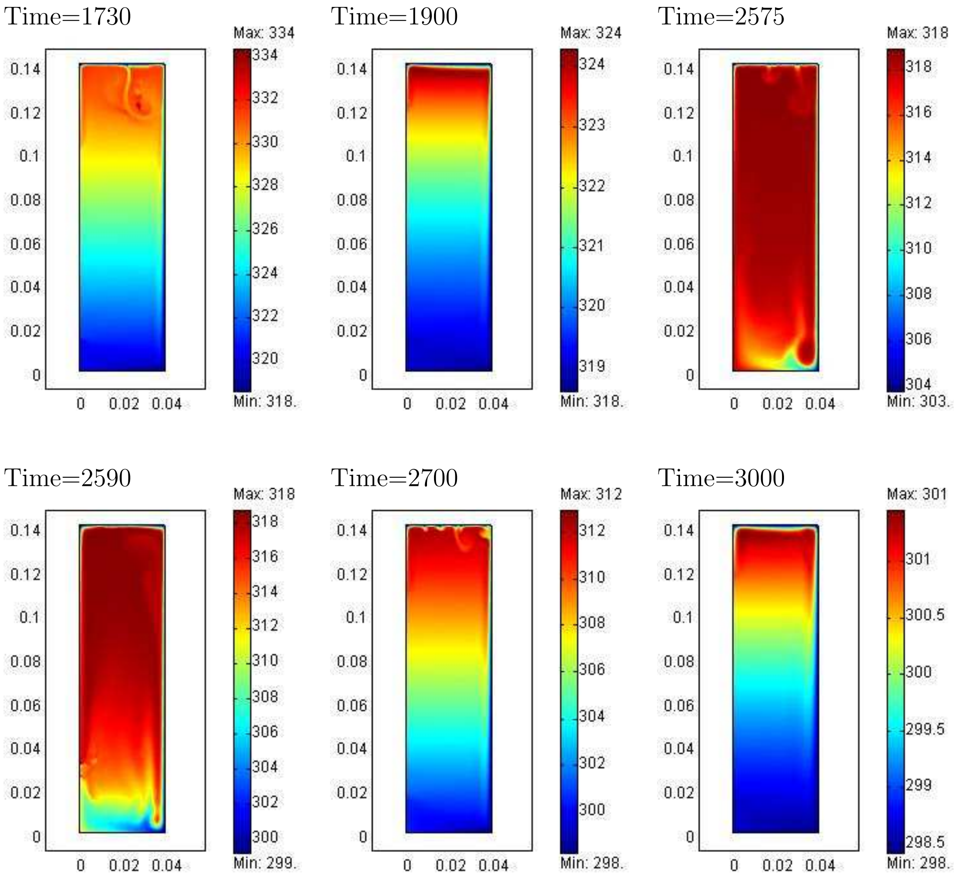

Time=1730 Time=1900 Time=2575

Time=2590 Time=2700 Time=3000

Figure 8.20: Temperatures in the large can for the times $t = 1730$, $t = 1900$, $t = 2575$, $t = 2590$, $t = 2700$ and $t = 3000$. Note that the temperature interval for each time is different.

On figure 8.21 and figure 8.22 the velocity fields are shown with arrows for the same times as the temperatures.

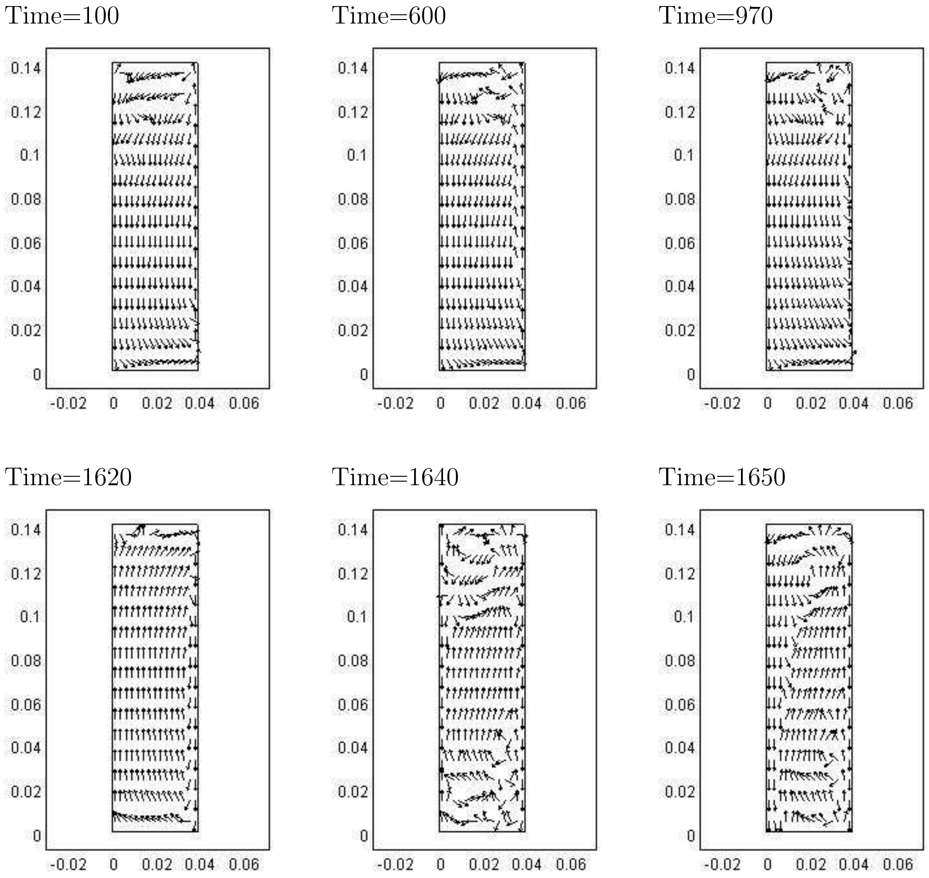
Time=100 Time=600 Time=970

Time=1620 Time=1640 Time=1650

Figure 8.21: Velocity field plotted with arrows in the large can for the times $t = 100$, $t = 600$, $t = 970$, $t = 1620$, $t = 1640$ and $t = 1650$.

The velocity fields for the large can also look very similar to the velocity field for the small can. In the heating zones the velocity field flows up along the side of the can and flows down in the middle. When the cooling begins the flow turns around and flows down along the side and up in the middle. In the beginning of the cooling zones substructures with opposing flows occurs in the top and bottom of the can. When the can has been in a cooling zone in a while the flow gets regular again with only small opposing flows in the top.

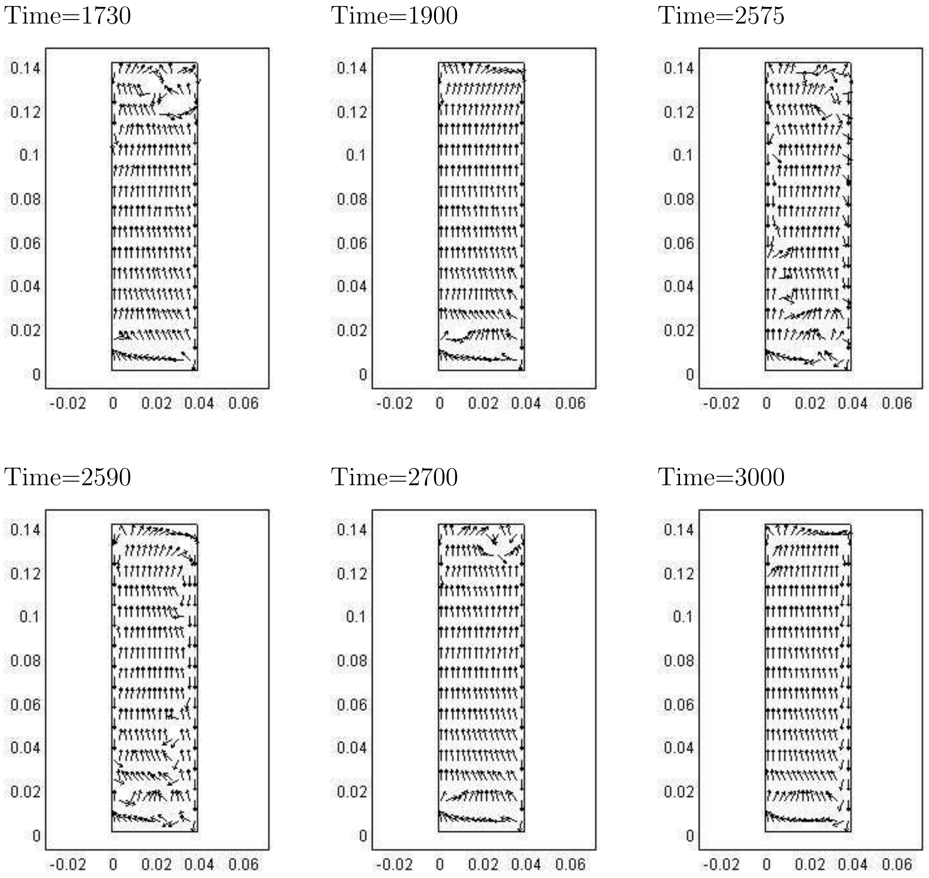

Time=1730 Time=1900 Time=2575

Time=2590 Time=2700 Time=3000

Figure 8.22: Velocity field plotted with arrows in the large can for the times $t = 1730$, $t = 1900$, $t = 2575$, $t = 2590$, $t = 2700$ and $t = 3000$.

On figure 8.23 and figure 8.23 the velocity fields are shown as contour plots for the same times as the temperatures and the velocity fields with arrows.

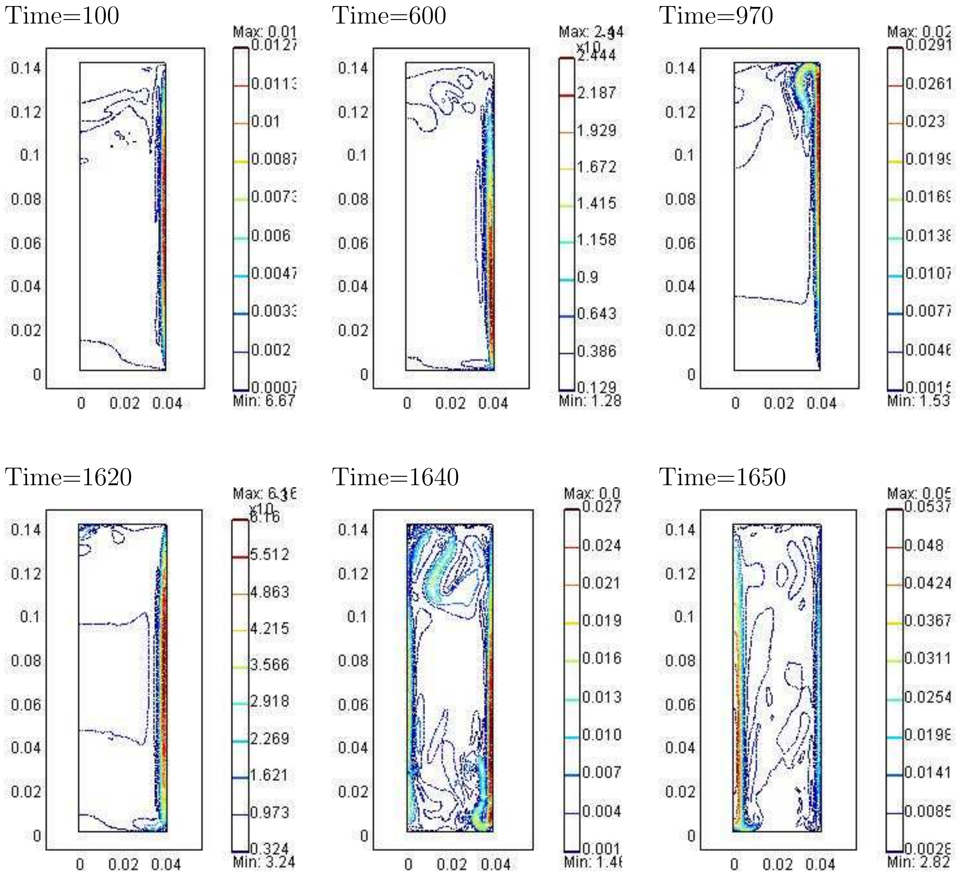
Time=100

Time=600

Time=970

Time=1620

Time=1640

Time=1650

Figure 8.23: Velocity field plotted as contour plot in the large can for the times $t = 100$, $t = 600$, $t = 970$, $t = 1620$, $t = 1640$ and $t = 1650$. Note that the velocity interval for each time is different.

The velocity fields as contour plot are made to show the order of the velocities. The maximum velocity on the plots is $5.4 \cdot 10^{-2} \frac{m}{s}$. As for the small can the velocity in the large can is largest near the side of the can during heating. During cooling the largest velocities are still near the side but also in the substructures with opposing flows.

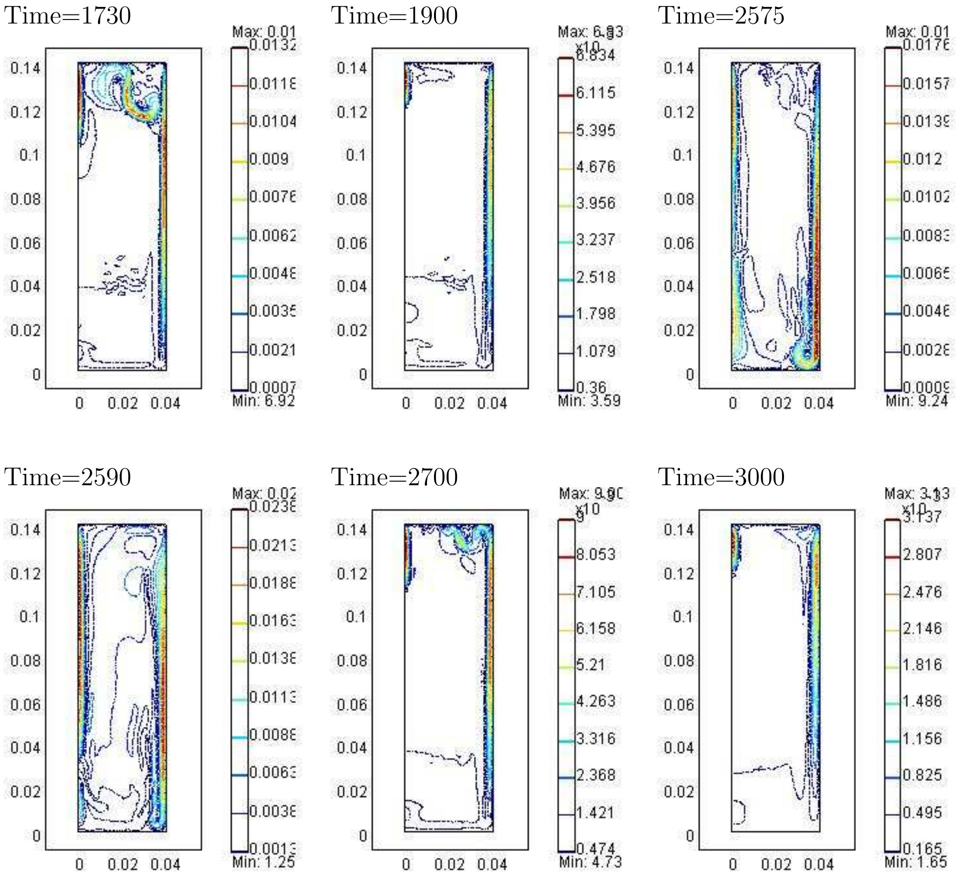

Figure 8.24: Velocity field plotted as contour plot in the large can for the times $t = 1730$, $t = 1900$, $t = 2575$, $t = 2590$, $t = 2700$ and $t = 3000$. Note that the velocity interval for each time is different.

8.3.3 Other results

There was made an attempt to make a model with air in the top of the cans. A small subdomain was drawn in the top of the can and the material coefficients for air from the material library in COMSOL was used on this subdomain. During this thesis it was not possible to solve this model in COMSOL.

A model of a glass "can" was made. A subdomain around the existing boundaries was drawn and the material coefficients for glass from COMSOL were used on this subdomain. The results were very similar to the results for the normal can without glass. The only difference was that the heat transfer was slower than for the normal can because the heat the cold had to go through the glass first. The results for the glass "can" are not shown because they are practically the same as the results for the cans.

8.3.4 Summary

The results for the small can, the large can and the glass ”can” are very similar. The only difference is the timescale. During the heating zones the product temperature increases regular from the top of the can to the bottom and the velocity field flows up along the side of the can and down in the middle. In the beginning of the cooling zones the flow turns around and flows down along the side and up in the middle. Very quickly this regular flow gets more irregular and substructures with opposing flow occurs. After a while in the cooling zones the flow again gets more regular and only small substructures with opposing flows occurs in the top of the can.

8.4 Investigation of the mean temperature

To get an idea of where in the container the mean temperature should be measured the solutions from COMSOL are used. When the product temperature is measured in the experiments this is always done in the middle of the container which corresponds to the symmetric axis.
The solution data on a 10×10 grid for each time from COMSOL is exported to MATLAB. From these data the mean temperatures T_{mean} for each time are found. Solution data on the axisymmetric boundary is also exported to MATLAB. These data corresponds to the product temperature T_p down in the middle of the container.
The differences between the mean temperature and the temperatures in the middle of the container are plotted as function of time with different colors depending on the height h, measured in cm from the bottom in the container where each temperature is found. The closer $T_{mean} - T_p$ is to 0 the closer T_p is to T_{mean}.
The result for the small can can be seen on figure 8.25.

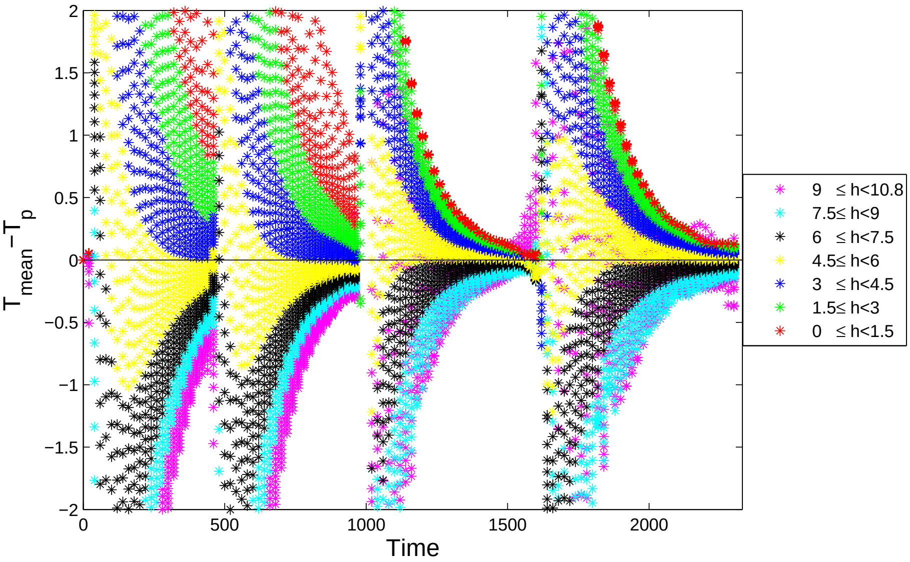

Figure 8.25: The difference between the mean temperature T_{mean} and the product temperature T_p in the middle of the small can.

The figure shows that $T_{mean} - T_p = 0$ lies in the yellow area almost all the time except for very small time periods which is in the beginning of each zone. In the end of zone 2 $T_{mean} - T_p = 0$ is on the boundary between the yellow and the blue area. The yellow area corresponds to $4.5 \leq h < 6$. The small can is $10.8cm$ high so $4.5 \leq h < 6$ is in the middle of the height of the can. If the mean product temperature should be measured the middle of the height would be a good place.

On figure 8.26 the result for the large can is shown. Note that the colors now correspond to different height intervals.

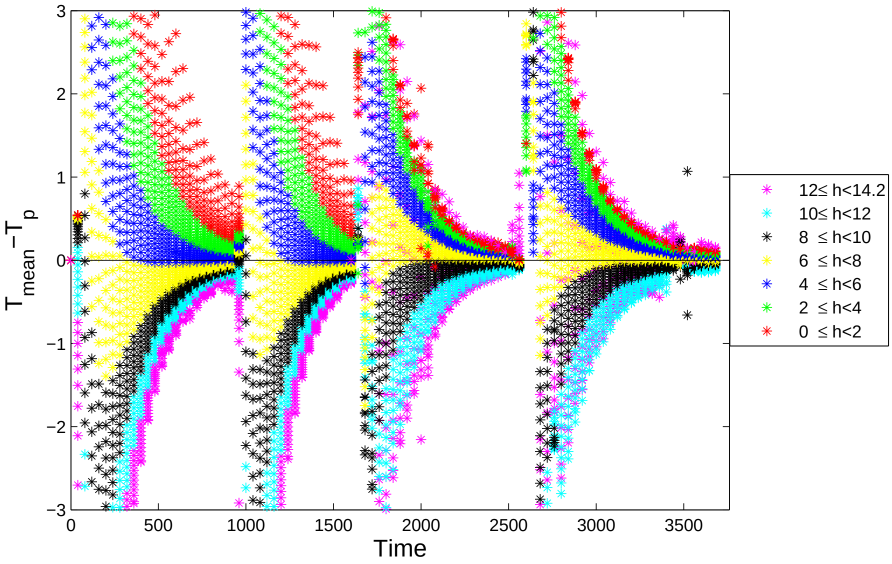

Figure 8.26: The difference between the mean temperature T_{mean} and the product temperature T_p in the middle of the large can.

The result on the figure is similar to the result for the small can. $T_{mean} - T_p = 0$ lies in the yellow area almost all the time except in the beginning of the zones. In the end of zone 1 and zone 2 $T_{mean} - T_p = 0$ is on the boundary between the yellow and the blue area. Also in the large can the mean product temperature should be measured in the middle of the height of the can.

As mentioned earlier there is air in the top of the real cans. This means that the mean product temperature should be measured in the middle of the height of the product in the can and not in the middle of the height of the can.

CHAPTER 9

Comparisons between measured data and results from COMSOL

The figures 5.1 and 5.8 which shows the measured product temperature as function of time from data sets and the figures 8.6 and 8.16 which shows the calculated product temperatures as function of time from COMSOL are very similar. They are all very regular during the heating zones and do all have leaps in the beginning of the cooling zones. The temperatures from COMSOL has more leaps than the measured temperature. The reason for this is that there is air in the top of the real can in the experiments but it was not possible to model this air in COMSOL during the work with this thesis. The air means that there is no contact between the can and the product in the top of the can and this causes that the heat transfer has to go through the air. The air insulates the water a little bit against the heat from the top.

Another difference on the two types of figures is that the product temperature down through the can varies more on the figures from COMSOL than on the figures made from the data sets. This is due to the fact that the models from COMSOL are made with values for water but the figures 5.1 and 5.8 are for cans with beer. On figure 5.20 the product temperature from a data set made in water is shown. On this figure the temperature down through the can also varies more than on the two figures for beer. So this difference is due to that values for water is used instead of values for beer.

The COMSOL model with glass gives almost the same results as without the glass. This is not what figure 5.15 from a bottle shows. This figure shows that the temperatures in the glass bottle do not make the leaps in the cooling zones. The difference between the experiment and the COMSOL model is due to that it was not possible to model the air in the top of the container. If this had been possible the glass would have made the heat transfer slower and the air would have insulated the product from the heat and cold. The results from a model with air and glass would probably have coincided with the result from figure 5.15.

Another difference on the results from COMSOL and the results from experiments is that axisymmetry is used in COMSOL. Because this is not exactly the case in the experiments in the pasteur, the results which appears on the axisymmetric boundary in COMSOL could appear anywhere in the container in the experiments.

Chapter 10

Relation to the regulation of the pasteurs and future work

The implementation of the models is stable and gives good results with a perturbation on 0.001 or smaller if the initial values for the coefficients are in the found intervals.
The new product model is better than the present product model but it should be taken in to the considerations that the new model is more sensitive to irregularities in the measurements in the data sets.
The new spray temperature in the gaps from function (6.1) should be implemented and tested in a real pasteur because it might give better results because the containers in the real pasteurs spend a larger part of the total time in the gaps.
The coefficients in the models dependency on the spray temperature level and the difference between the spray temperature in two neighboring zones should be implemented to see if the results are better than before.
The mean product temperature can be measured in the middle of the height of the product in the cans.
The substructure with opposing flows which appears during the cooling zones means that the product gets cooled bit faster than expected because the is more flow in the product.

Chapter 11

Conclusion

In this thesis the implementation of two product models was examined. The perturbation which is used to find the Jacobian matrix in the implementation was investigated and it was found that the value used in the preproject, was a good perturbation because it gave good result. If the value is larger, the new product model gives bad results. The value can be smaller for both models. So as long as the perturbation is equal to or smaller than the found value the implementation of both models gives good and reliable results.

The initial values for the coefficients in both models were tested and intervals for each initial value were found. When the initial values for the coefficients are inside these intervals the results from the implementation are reliable.

The initialization of the two models in the implementation was also tested. Before the test the implementation gave the same product temperature in the first step as the initial product temperature. The reason for this was found and a new implementation of both models was tested. For the present product model there was no change in the results. For the new model the results with the new implementation was bad. Therefore the initialization and the implementation should be maintained.

The spray temperature which the container experiences while being transported through the pasteur was examined. In the spray zones the current spray temperature coincided with the measured temperature. In the gaps a new modelled spray temperature was tested for both models. The new spray temperature in the gaps basically gave the same results as the other spray temperature in the gaps. This is because the container spends very short time in each gap in relation to the time it spends in the spray zones.

The coefficients dependency on the spray temperature level and the difference between the spray temperature in two neighboring zones was analyzed. The model coincided very bad with the data sets in the cooling zones so the available data sets were inappropriate to this investigation. For both models in the heating zones it was found that c_1 has a linear dependency on ΔT but does not depend on the spray temperature level, c_2 depends on the spray temperature level but does not have a dependency on ΔT. For the new model the coefficients c_8 and c_9 neither have a dependency on the spray temperature level nor ΔT.

The flow and the temperature during the pasteurization were investigated. During the heating zones the flow and temperature behaved as expected. The flow and temperature showed some unknown phenomena during the cooling zones with some substructures with opposing flows. These unknown phenomena were verified by experiments. The mean product temperature was found to be in the middle of the height of the product in the cans almost all the time so this would be a good place to measure in mean product temperature.

Thus it can be concluded that all purposes of this thesis were investigated and that much greater knowledge about the pasteurization process is achieved. It proved possible to improve the existing models and it should thereby be possible to make a better regulation of the pasteurs.

References

[1] EBC Technology & Engineering Forum: *Beer Pasteurisation*, Getränke-Fachverlag, (1995)

[2] V.A.Barker and J.Reffstrup: *The Finite Element Method for Partial Differential Equations*, Notes, (1998)

[3] C.A.J.Fletcher: *Computational Techniques for Fluid Dynamics*, vol. 2, Springer Verlag, Berlin (1988)

[4] N. Asmar: *Partial Differential Equations and Boundary Value Problems*, Prentice Hall, New Jersey, (2000)

[5] L.F.Shampine, R.C.Allen, Jr and S.Pruess: *Fundamentals of Numerical Computing* John Wiley & Sons, Inc., USA, (1997)

[6] W.J.Palm III: *Introduction to MATLAB 6 for Engineers*, 1st ed., McGraw-Hill Companies, Inc., Singapore, (2001)

[7] Arfken and Weber: *Mathematical Methods for Physicists*, Academic Press, USA, 5. edition (2001)

[8] COMSOL manual: *COMSOL Multiphysics User's Guide*, 1. ed., COMSOL AB, (2005)

[9] COMSOL manual: *COMSOL Multiphysics Modeling Guide*, 1. ed., COMSOL AB, (2005)

[10] David R.Lide (Editor-in-chief): *CRC Handbook of chemistry and physics 1993-1994*, Special student edition, 74. ed., CRC Press, Boca Raton, Florida

[11] http://www.formel.dk/materialedata/glas.htm

[12] http://www.mathworks.com/access/helpdesk/help/techdoc/ref/mean.html

[13] http://www.mathworks.com/access/helpdesk/help/techdoc/ref/std.html

[14] http://www.mathworks.com/access/helpdesk/help/techdoc/ref/var.html

[15] http://www.mathworks.com/access/helpdesk/help/techdoc/ref/lsqr.html